NASA CONTRACTOR REPORT

NASA CR-13
c. 1

NASA CR-1331

SOME OPTIMAL BRANCHED TRAJECTORIES

by Joseph D. Mason

Prepared by
TRW SYSTEMS GROUP
Redondo Beach, Calif.
for Langley Research Center

NATIONAL AERONAUTICS AND SPACE ADMINISTRATION • WASHINGTON, D. C. • MAY 1969

NASA CR-1331

SOME OPTIMAL BRANCHED TRAJECTORIES

By Joseph D. Mason

Prepared under Contract No. NAS 1-8011 by
TRW Systems Group
Redondo Beach, Calif.

for Langley Research Center

NATIONAL AERONAUTICS AND SPACE ADMINISTRATION

For sale by the Clearinghouse for Federal Scientific and Technical Information
Springfield, Virginia 22151 – CFSTI price $3.00

ABSTRACT

This paper carries out a study of optimal branched trajectories. Branched trajectories are a class of trajectories that includes the motion of several vehicles which travel united for some time and then break apart in order to proceed individually to separate end conditions. The problem is transformed to the classical variational problem of Bolza by several linear transformations of time. At this point the established necessary minimizing conditions of optimal control theory may be applied. A number of applications are considered and numerical solutions are obtained in two cases.

FOREWORD

This report was prepared by the TRW Systems Group of TRW Inc., One Space Park, Redondo Beach, California. It represents the final documentation of a study of optimum branched trajectories under contract NAS1-8011. The contract was administered by the National Aeronautics and Space Administration with John D. Bird of the Langley Research Center acting as technical monitor.

This study resulted from a proposal by TRW Systems Group for research on optimal branched trajectories. The work began in April 1968 and was completed in December 1968. Dr. Joseph D. Mason was principal investigator. The work was performed under the direction of Mr. P. Steiner, Manager of the Guidance and Analysis Department, and Mr. C. G. Pfeiffer, Head of the Mathematical Physics Section.

SOME OPTIMAL BRANCHED TRAJECTORIES

By Joseph D. Mason
TRW Systems Group

SUMMARY

The application of modern optimization techniques to aerospace trajectory design and guidance development has previously been limited to two classes. First, optimal trajectories have been determined for individual vehicles with a single mission. Second, the trajectories for two or more vehicles engaged in a cooperative or contradictory game have been examined. Mathematical techniques such as the calculus of variations have been successfully applied to some problems of the first group while the development of the theory of differential games has provided a method of solution for some multiple vehicle problems.

A third group of aerospace trajectories which is an outgrowth of the variational treatment of single vehicle motion may be categorized as branched trajectories. This class includes the motion of several vehicles which travel united for some time and then break apart in order to proceed individually to separate end conditions.

If a single performance index can be stated for a branched trajectory then the optimization problem can be converted to a conventional optimal control problem of Bolza by means of several linear transformations of time. Using this approach the well established necessary minimizing conditions of optimal control theory can be applied directly to the branched trajectory problem.

The particular applications considered include a variety of conceptually different problems. First, the insertion of two payloads into separate orbits with a single launch vehicle is examined. The optimal staging of such a vehicle is also treated. Next, a method of designing launch trajectories based on abort (or alternate mission) capability is presented. This method permits fixing the primary mission performance while improving the ability to abort in case of failure. Branched maneuvers of lunar lander/orbiter vehicles are also examined as are cooperative multiple aircraft maneuvers.

Numerical solutions for the two payload launch and the abort problem are presented. These solutions demonstrate the feasibility and wide applicability of optimal branched trajectory theory.

1.0 INTRODUCTION

Consider the trajectory design for a multistage rocket having the capability of deploying several upper stages simultaneously and the mission of inserting, with each upper stage, a fixed payload into orbit. Such a trajectory is represented by Figure 1. As indicated this trajectory consists of four segments called branches. The first stage burns along branch 1 and the empty stage is discarded at point B. The upper stages ignite at B and proceed along branches 2,3 and 4 respectively. Three payloads are inserted into three separate orbits at points P_1, P_2 and P_3. If each of the three payloads is fixed then the trajectory design and stage sizing might be based on minimizing initial weight (at point L).

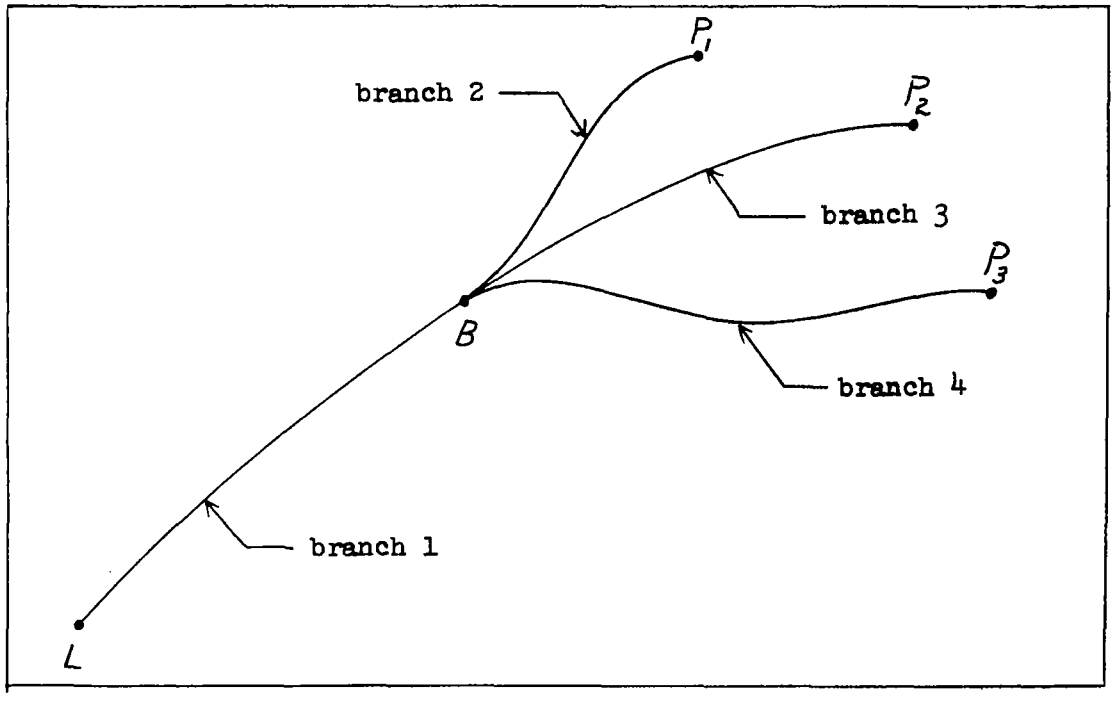

FIGURE 1. A Multiple Payload Trajectory

Trajectories of the type just described are typical of a much larger class known as branched trajectories. They differ from conventional trajectories in that the state and control dimensions vary (discretely) with time. Also, in the most general case, the end points of each of the branches are related through imposed terminal and intermediate boundary conditions.

In mathematical terms a branch is defined by a pair of parameters a^j, b^j with $b^j > a^j$, a continuous n-dimensional state vector $x^j(t)$ and a piecewise continuous q-dimensional control vector $u^j(t)$ with $a^j \le t \le b^j$. Each branch will be identified by the index $j = 1, \ldots, m$. On the j-th branch the state and control are constrained by differential equations plus algebraic equations and inequalities; i.e.

$$\dot{x}^j = f^j[x^j, u^j, t]$$

$$\phi_\alpha{}^j[x^j, u^j, t] = 0 \qquad \alpha = 1, \ldots, r$$

$$\phi_\alpha{}^j[x^j, u^j, t] \le 0 \qquad \alpha = r+1, \ldots, s.$$

This description will be appropriately modified in the formal treatment of the following section.

With this concept of a branch, a branched trajectory E, may be described as a set of m branches whose endpoints satisfy a set of boundary conditions,

$$g_e[x^1(a^1),\ a^1,\ x^1(b^1), b^1, \ldots, x^m(a^m), a^m, x^m(b^m), b^m] = 0.$$

Among those branched trajectories, E, one which minimizes a performance function

$$J = g_o[x^1(a^1), a^1, x^1(b^1), b^1, \ldots, x^m(a^m), a^m, x^m(b^m), b^m] + \sum_{j=1}^{m} \int_{a^j}^{b^j} f_o{}^j[x^j, u^j, t]\, dt$$

is called a minimal branched trajectory, E_o.

Optimal branched trajectories might best be characterized as belonging to the larger class of discontinuous variational problems. For this reason a brief sketch of the early history of such problems is in order.

As early as 1906 Bliss and Mason (ref. 1) considered a Lagrange-type problem in the calculus of variations for which the integrand experiences a finite discontinuity on a given curve. Such a problem is encountered in the investigation of light rays in a medium having refracting surfaces. Generalizations of this problem were presented by Roos (ref. 2) in 1929 and Graves (ref. 3) in 1930.

Perhaps the first solution which could properly be called an optimal branched trajectory was given by Sinclair (ref. 4) in 1909. She examined a soap bubble problem for which the solution is made up of three surfaces of revolution whose generating curves are connected at a common point. This example will be discussed in a later section.

The transformation to be used in converting the branched trajectory to a conventional Bolza form was used by Denbow (ref. 5) in 1937 for a continuous Bolza problem with intermediate boundary conditions. The same transformation was used in 1930 by Hestenes (ref. 6) to convert a problem with free final value for the independent variable to one of the fixed type.

The results of Denbow have recently been revised by Hunt and Andrus (ref. 7) to account for fixed discontinuities at the intermediate boundaries and by Mason, Dickerson and Smith (ref. 8) to account for variable or functional discontinuities. Also, Boyce and Linnstaedter (ref. 9) have revised Hunt's results for control problems with inequality constraints. All of these works (refs. 5, 7, 8, and 9) were summarized and reviewed by Burns (ref. 10).

The reasons for using the transformation approach both in the past and for branched trajectories are the same. The transformation is conceptually simple in comparison with all the intricacies of a complete variational treatment. Once the problem has undergone the transformation a rather complete set of necessary conditions is readily available. On the other hand, if a heuristic approach is desirable, then it is advisable to attack the branched trajectory problem directly with classical variations; such a treatment was performed by Vincent (ref. 11).

Those aerospace trajectory problems examined in this study by no means exhausts the utility of optimal branched trajectories. However, they are considered to be typical of the expected future applications. Particular acknowledgement must be given to W. D. Dickerson and D. B. Smith of TRW Systems Group for their contributions to many aspects of this study and for their development of the terminal aircraft traffic control problem.

2.0 SOME NECESSARY CONDITIONS

The more conventional form of deterministic optimal control problems, referred to as the "ordinary differential" type by Warga (ref.12), constitutes the basis for many of the recent developments in mathematical control theory. The usual state and control variables for such problems are defined on a closed time interval and related on that interval by a set of differential and algebraic equations. Unfortunately, many applications, especially in the field of aerospace trajectory optimization, are not easily treated as a conventional form.

For example, consider the optimal steering of a multi-stage rocket which has the capability of separating into several self-propelled stages each proceeding independently to accomplish its own mission. The performance of each mission may depend not only on the steering program but also on the location in state-time space of the separation point. For the purposes of this paper the trajectory of each stage will be referred to as a branch and the composite of all branches will be called a branched trajectory.

This work presents a generalization of conventional results to the case of optimal control problems made up of several branches which themselves are unrelated except through boundary conditions and a single performance function. The approach taken here to establish a useful set of necessary conditions is to transform the multiple branches into a conventional form which Hestenes (ref. 13) calls a general control problem of Bolza. This technique is a modification of the work by Denbow (ref. 5) and others. Since necessary conditions for the conventional problem are well known, the remaining task is merely one of inverting the transformation thereby carrying the necessary conditions into the multiple-branch format.

PROBLEM FORMULATION. Let a^j, b^j be a pair of parameters such that

$$b^j > a^j, \quad j = 1, \ldots, m.$$

Let

$$x^j(t), \quad a^j \leq t \leq b^j,$$

be an n-dimensional continuous state vector and

$$u^j(t), \quad a^j \leq t \leq b^j,$$

a q-dimensional piecewise continuous control vector. The superscript j, denotes the branch; e.g.

$$x^2 = [x_1^2, x_2^2, \ldots, x_n^2]$$

is the state vector on the second branch.

Let

$$f^j[x^j(t), u^j(t), t]$$

be an n-dimensional vector valued function,

$$\phi^j[x^j(t), u^j(t), t]$$

an s-dimensional vector valued function, and

$$f_o{}^j[x^j(t), u^j(t), t]$$

a scalar function with all of these functions of class C' on a region R^j of x^j-u^j-t Euclidean (n+q+1) - space (see ref. 13).

A branch, E^j, is defined as the pair of parameters a^j, b^j and functions

$$x^j(t), u^j(t)$$

satisfying differential equations of the form

$$\dot{x}^j = f^j[x^j, u^j, t] \tag{2.1}$$

and relations

$$\phi_\alpha{}^j[x^j, u^j, t] = 0 \qquad \alpha = 1, \ldots, r \tag{2.2}$$

and

$$\phi_\alpha{}^j[x^j, u^j, t] \leq 0 \qquad \alpha = r+1, \ldots, s \tag{2.3}$$

which define $R_o{}^j \subset R^j$.

The functions $\phi^j[x^j, u^j, t]$ are further restricted to those functions for which the matrices

$$\left(\frac{\partial \phi_\alpha{}^j}{\partial u_k{}^j}\right) \qquad \begin{matrix} \alpha = \alpha_1, \ldots, \alpha_{d^j} \\ k = 1, \ldots, q \end{matrix} \tag{2.4}$$

have rank d^j at points $\bar{x}^j, \bar{u}^j, \bar{t}$ in R_o^j where $\alpha_1, \ldots, \alpha_{d^j}$ are the indices on the range 1, ..., s for which

$$\phi_\alpha{}^j[\bar{x}^j, \bar{u}^j, \bar{t}] = 0. \tag{2.5}$$

This restriction insures that each of equations (2.5) determines one component of the control vector.

Let x_a represent the set of all $x^j(a^j)$, x_b the set of all $x^j(b^j)$, a the set of all a^j and b the set of all b^j, $j = 1, \ldots, m$. Also let $g_o[x_a, x_b, a, b]$ be a salar function and $g[x_a, x_b, a, b]$ be a p-dimensional vector valued function. These functions are defined on a domain B which is a subset of (2mn+2m)-dimensional Euclidean space and $p < (2mn + 2m)$.

A branched trajectory, E, may now be defined as a set of m branches whose endpoints satisfy the boundary conditions

$$g[x_a, x_b, a, b] = 0. \tag{2.6}$$

Among all possible branched trajectories, E, one which minimizes

$$J = g_o[x_a, x_b, a, b] + \sum_{j=1}^{m} \int_{a^j}^{b^j} f_o{}^j[x^j, u^j, t]\, dt \tag{2.7}$$

is called a minimal branched trajectory and denoted by E_o.

For purposes of analysis the previous definitions will be modified to include only functions g_o and g which are of class C' in a neighborhood of the values x_a, x_b, a, b pertaining to E_o.

An optimal control problem with multiple branches is that of finding a minimal branched trajectory, E_o, as defined above. Only certain necessary conditions for E_o will be established here.

THE TRANSFORMATION. In order to obtain minimizing conditions for the above problem a transformation (ref. 5) will be applied to convert the m-branch problem to a conventional single-branch control problem of Bolza (ref. 13). On the j-th branch change the independent variable from t to T according to the relation

$$t = a^j + (b^j - a^j)\, T \qquad a^j \le t \le b^j \tag{2.8}$$

$$0 \le T \le 1.$$

As shown in Figures 2 and 3 the individual branches of a typical branched trajectory are defined over different intervals of the t-domain but they are all defined on the interval [0,1]in the T-domain.

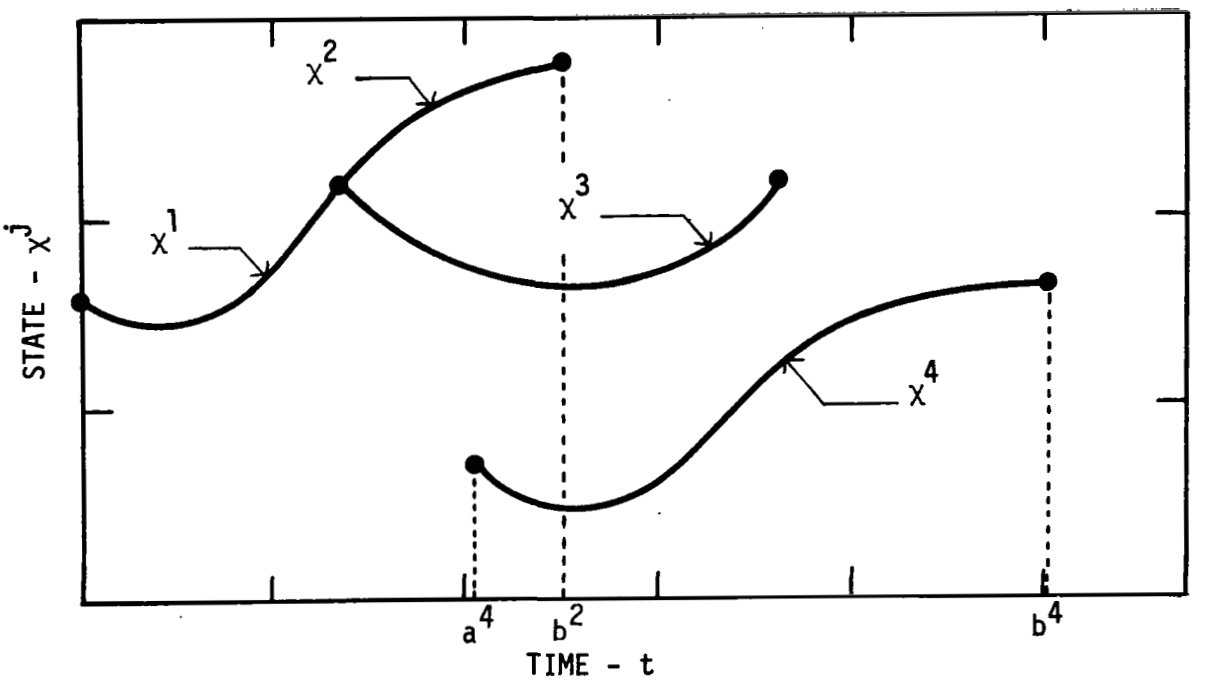

Figure 2. Typical 4-Branch Trajectory in State-t Space

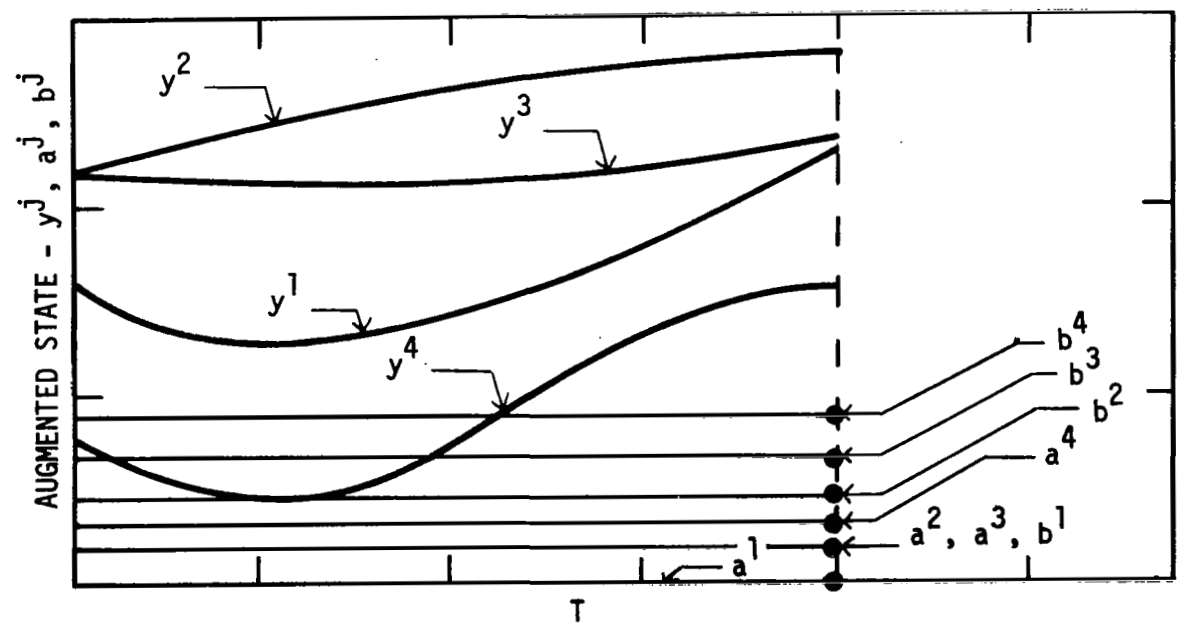

Figure 3. Typical 4-Branch Trajectory in Augmented State-T Space

In order to maintain a one-to-one relationship between t and T it is necessary that $a^j \neq b^j$. This restriction rules out null branches as possible components of E_o and constitutes a severe limitation which must be taken into account for most applications.

Under the change of independent variable the state $x^j(t)$ and control $u^j(t)$, defined on the range $a^j \leq t \leq b^j$, respectively become new variables $y^j(T)$ and $v^j(T)$ defined on the range $0 \leq T \leq 1$. Thus, applying the transformation successively for $j = 1, \ldots, m$ the range of each of the m vectors $x^j(t)$ and the m vectors $u^j(t)$ is mapped onto the closed interval $[0,1]$. The notation $y(T)$ will be used to indicate the set of all vectors $y^j(T)$, $j = 1, \ldots, m$ and, similarly, $v(t)$ will be the set $v^j(T)$, $j = 1, \ldots, m$.

The functions

$$f^j[x^j, u^j, t]$$

are transformed to

$$h^j[y^j, a^j, b^j, v^j, T]$$

where the a^j and b^j appear now explicitly in the form dictated by equation (2.8). The functions ϕ^j are similarly transformed to ψ^j so that relations (2.1), (2.2) and (2.3) become:

$$\frac{dy^j}{dT} = (b_j - a_j)\, h^j[y^j, a^j, b^j, v^j, T] \tag{2.9}$$

$$\psi_\alpha{}^j[y^j, a^j, b^j, v^j, T] = 0 \qquad \alpha = 1, \ldots, r \tag{2.10}$$

$$\psi_\alpha{}^j[y^j, a^j, b^j, v^j, T] \leq 0 \qquad \alpha = r+1, \ldots, s \tag{2.11}$$

Since the parameters a^j, b^j now appear in these equations they will be treated as constant state variables, their constancy being indicated by the additional differential equations

$$\frac{da}{dT} = 0 \tag{2.12}$$

and

$$\frac{db}{dT} = 0. \tag{2.13}$$

Where the parameters a,b originally appeared in the functions g_o and g, they will now appear as a(o),b(o) in keeping with their new status.

as state variables. This convention is a matter of choice; a(1) could be used in place of a(o), etc. Thus, the values of a and b are free except as constrained by equations (2.14) below.

The boundary conditions (2.6) and the performance criterion (2.7) become, under the transformation,

$$g[y(o),y(1),a(o),b(o)] = 0 \tag{2.14}$$

and

$$I = g_o[y(o),y(1),a(o),b(o)] + \int_o^1 \sum_{j=1}^{m} (b^j - a^j)\, h_o{}^j[y^j,a^j,b^j,v^j,T]\, dT. \tag{2.15}$$

The right sides of equations (2.9), (2.12) and (2.13), the left sides of relations (2.10) and (2.11) and the integrand of (2.15) are all of class C' on a domain S of $|m(n+q)+2m+1|$-dimensional Euclidean space. The relations (2.10) and (2.11) define S_o, a subset of S.

Let $\psi[y,a,b,v,T]$ be the set of all $\psi^j[y^j,a^j,b^j,v^j,T]$, $j = 1, \ldots, m$ so that from the previous assumptions concerning $\phi^j[x^j,u^j,t]$, the matrix

$$\frac{\partial \psi}{\partial v} \quad \text{has rank} \quad c = \sum_{j=1}^{m} d^j$$

at points $\bar{y},\bar{a},\bar{b},\bar{v},\bar{T}$ in S_o with components $\bar{y}^j,\bar{a}^j,\bar{b}^j,\bar{v}^j,\bar{T}$ satisfying

$$\psi_\alpha{}^j[\bar{y}^j,\bar{a}^j,\bar{b}^j,\bar{v}^j,\bar{T}] = 0$$

for $\alpha = \alpha_1, \ldots, \alpha_{d^j}$.

SOME NECESSARY CONDITIONS. A trajectory, E*, for the transformed problem is a (mn+2m)-dimensional continuous state vector, $z(T) \supset y(T)$, a(T), b(T), and an (mq)-dimensional piecewise continuous control vector, v(T), which satisfy relations (2.9) through (2.13) and whose endpoints satisfy equations (2.14). A minimal trajectory, E_o^* $|$with components $z_o(T),v_o(T)|$, for the transformed problem is one of the E* which minimizes I. Necessary conditions for a minimal trajectory E_o^* have been established by Hestenes (ref. 13) and will be stated here without proof.

Theorem 1. Let E_o^* be a minimal trajectory for the transformed problem just described. There exist multipliers $\lambda_o \geq 0$ and

$$\Lambda_i{}^j(T), \Gamma_j{}^a(T), \Gamma_j{}^b(T), M_\alpha{}^j(T), \varepsilon_e$$

$(j = 1, \ldots, m;\quad i = 1, \ldots, n;\quad \alpha = 1, \ldots, s;\quad e = 1, \ldots, p)$

not vanishing simultaneously, and functions*

$$K^j[y^j, a^j, b^j, v^j, \Lambda^j, M^j, T] = \Lambda^j \cdot h^j - \lambda_o h_o{}^j - M^j \cdot \psi^j, \tag{2.16}$$

$$K[z, v, \Lambda, M, T] = \sum_{j=1}^{m} (b^j - a^j)\, K^j \tag{2.17}$$

and

$$F[z(o), z(1)] = \lambda_o g_o[y(o), y(1), a(\cdot), b(o)] + \varepsilon \cdot g[y(o), y(1), a(o), b(o)] \tag{2.18}$$

such that

(i) The multipliers $M^j(T)$ are piecewise continuous on $0 \le T \le 1$ and are continuous at each point of continuity of $v_o{}^j(T)$. Moreover,

$$M_\alpha{}^j(T) \ge 0 \quad (r+1 \le \alpha \le s)$$

with $M_\alpha{}^j(T) = 0$ at each value of T at which

$$\Psi_\alpha{}^j[y_o{}^j(T), a_o{}^j(T), b_o{}^j(T), v_o{}^j(T), T] < 0,$$

(ii) The multipliers $\Lambda(T)$, $\Gamma^a(T)$ and $\Gamma^b(T)$ are continuous and have piecewise continuous derivatives while the functions

$$z_o(T), v_o(T), \Lambda(T), M(T)$$

satisfy the Euler-Lagrange equations

$$\frac{dy^j}{dT} = (b^j - a^j)\, K^j_{\Lambda^j} \tag{2.19}$$

$$\frac{da}{dT} = K_{\Gamma^a} = 0 \tag{2.20}$$

---

*The dot separating two vectors indicates an inner or scalar product:

$$\Lambda^j \cdot h^j = \sum_{i=1}^{n} \Lambda_i{}^j h_i{}^j$$

(2.21) $$\frac{db}{dT} = K_{\Gamma^b} = 0$$

(2.22) $$\frac{d\Lambda^j}{dT} = -(b^j - a^j)\, K^j_{y^j}$$

(2.23) $$\frac{d\,\Gamma^a_j}{dT} = K^j - (b^j - a^j)\, K^j_{a^j}$$

(2.24) $$\frac{d\Gamma^b_j}{dT} = -K^j - (b^j - a^j)\, K^j_{b^j}$$

(2.25) $$K^j_{v^j} = 0$$

(2.26) $$\frac{dK^j}{dT} = K_T{}^j \qquad\qquad J = 1, \ldots, m$$

on each interval of continuity of $v_o{}^j(T)$. The functions

$$K^j[y_o{}^j(T), a_o{}^j(T), b_o{}^j(T), \Lambda^j(T), M^j(T), T]$$

are continuous on $0 \le T \le 1$ and the transversality condition

(2.27) $$dF + [\Lambda^j(T) \cdot dy^j(T) + \Gamma^a(T) \cdot da(T) + \Gamma^b(T) \cdot db(T)]_{T=0}^{T=1} = 0$$

holds on E_o^* for all $dz(o)$ and $dz(1)$.

(iii) The inequality

(2.28) $$K[z_o(T), v, \Lambda(T), 0, T] \le K[z_o(T), v_o(T), \Lambda(T), 0, T]$$

holds for all $(z_o(T), v, T)$ in S_o.

This Theorem in its present form could be used to investigate solutions of branched trajectory problems directly. However, due to the large dimensionality of the transformed problem it seems reasonable to invert the transformation thereby obtaining a corollary of Theorem 1 given in terms of the original problem statement.

Since each function of T in Theorem 1 carries (perhaps implicitly) an index j, it is possible to apply the inverse of (2.8) for each value of j on the range 1, ..., m. Under this operation the multipliers $\Lambda^j(T)$ become $\lambda^j(t)$ and the multipliers $M^j(T)$ become $\mu^j(t)$. Therefore, the functions defined by (2.16) and (2.18) become

$$H^j[x^j(t),u^j(t),\lambda^j(t),\mu^j(t),t] = \lambda^j \cdot f^j - \lambda_o f_o{}^j - \mu^j \cdot \phi^j \tag{2.29}$$

and

$$G[x_a,x_b,a,b] = \lambda_o g_o[x_a,x_b,a,b] + \varepsilon \cdot g[x_a,x_b,a,b]. \tag{2.30}$$

A minimal trajectory, E_o^*, becomes a minimal branched trajectory, E_o, whose branches, E_o^j, have components

$$a_o{}^j, b_o{}^j \text{ and } x_o{}^j(t), u_o{}^j(t) \text{ on } a_o{}^j \le t \le b_o{}^j.$$

Condition (i) of Theorem 1 implies that the multipliers $\mu^j(t)$ are piecewise continuous on $a_o{}^j \le t \le b_o{}^j$ and are continuous at each point of continuity of $u_o{}^j(t)$. Moreover,

$$\mu_\alpha{}^j(t) \ge 0 \quad (r+1 \le \alpha \le s)$$

with

$$\mu_\alpha{}^j(t) = 0$$

at each value of t at which

$$\phi_\alpha{}^j[x_o{}^j(t),u_o{}^j(t),t] < 0.$$

Equations (2.19), (2.22), (2.25) and (2.26) of condition (ii) are readily transformed to:

$$\dot{x}^j = H^j_{\lambda^j} \tag{2.31}$$

$$\dot{\lambda}^j = -H^j_{x^j} \tag{2.32}$$

$$H^j_{u^j} = 0 \tag{2.33}$$

$$H^j = H_t{}^j \tag{2.34}$$

Equations (2.20) and (2.21) merely express the constancy of a and b and need not be transformed explicitly.

By making some observations equations (2.23) and (2.24) can be integrated immediately. Due to the specific appearance of a^j, b^j and T in the functions K^j

$$(b^j - a^j)\, K^j_{a^j} = (1 - T)\, K_T{}^j$$

and

$$(b^j - a^j)\, K^j_{b^j} = T K_T{}^j.$$

Now, taking (2.26) into account equation (2.23) can be written as

$$\Gamma_j{}^a(1) = \Gamma_j{}^a(o) + \int_o^1 \left[K^j - (1 - T)\, \frac{dK^j}{dT} \right] dT$$

or

$$\Gamma_j{}^a(1) = \Gamma_j{}^a(o) + K^j(o). \tag{2.35}$$

Similarly, equation (2.24) leads to

$$\Gamma_j{}^b(1) = \Gamma_j{}^b(o) - K^j(1). \tag{2.36}$$

The boundary values for Γ^a and Γ^b are determined by the transversality condition (2.27).

$$\Gamma^a(o) = \frac{\partial F}{\partial a(o)}$$

$$\Gamma^b(o) = \frac{\partial F}{\partial b(o)}$$

$$\Gamma^a(1) = \Gamma^b(1) = 0$$

Combining these results with equations (2.35) and (2.36) and using

$$H^j(a^j)$$

to represent

$$H^j[x^j(a^j), u^j(a^j), a^j],$$

$$\frac{\partial G}{\partial a^j} + H^j(a^j) = 0 \tag{2.37}$$

and

(2.38) $$\frac{\partial G}{\partial b^j} - H^j(b^j) = 0.$$

The remaining information contained in the transversality condition becomes

(2.39) $$\frac{\partial G}{\partial x^j(a^j)} - \lambda^j(a^j) = 0$$

and

(2.40) $$\frac{\partial G}{\partial x^j(b^j)} + \lambda^j(b^j) = 0.$$

Finally, for condition (iii) inequality (2.28) must hold for all points $z_o(T),v,T$ in S_o. Hence, it must hold for the choice

$$v^j = v_o{}^j(T) \text{ for } j = 1, \ldots, k-1, k+1, \ldots, q.$$

Since $b^j \geq a^j$, inequality (2.28) implies that

(2.41) $$H^j[x_o{}^j(t),u^j,\lambda^j(t),0,t] \leq H^j[x_o{}^j(t),u_o{}^j(t),\lambda^j(t),0,t]$$

must hold for all points

$$x_o{}^j(t),u^j,t \text{ in } R_o{}^j.$$

The preceding manipulations of Theorem 1 are summarized below for convenience.

Theorem 1-A. Let E_o be a minimal branched trajectory. There exist multipliers $\lambda_o \geq 0$ and

$$\lambda_i{}^j(t),\ \mu_\alpha{}^j(t),\ \varepsilon_e$$

$$(j = 1, \ldots, m;\ i = 1, \ldots, n;\ \alpha = 1, \ldots, s;\ e = 1, \ldots, p)$$

not vanishing simultaneously*. There also exist functions defined by (2.29) and (2.30) such that

*i.e., there exists no parameter σ on $0 \leq \sigma \leq 1$ such that, if $\sigma^j = a^j + (b^j - a^j)\sigma$, then λ_o, $\lambda^j(\sigma^j)$ and ε are all zero.

(a.) The multipliers $\mu_\alpha{}^j(t)$ are piecewise continuous on $a_o{}^j \le t \le b_o{}^j$ and are continuous at each point of continuity of $u_o{}^j(t)$. Moreover,

$$\mu_\alpha{}^j(t) \ge 0 \ (r+1 \le \alpha \le s) \text{ with } \mu_\alpha{}^j(t) = 0$$

at each value of t at which

$$\phi_\alpha{}^j[x_o{}^j(t),\ u_o{}^j(t),t] < 0.$$

(b.) The multipliers $\lambda^j(t)$ are continuous and have piecewise continuous derivatives. The functions

$$x_o{}^j(t), u_o{}^j(t), \mu^j(t)$$

satisfy equations (2.31) through (2.34) on each interval of continuity of $u_o{}^j(t)$. The functions

$$H^j[x_o{}^j(t), u_o{}^j(t), \lambda^j(t), \mu^j(t), t]$$

are continuous on $a_o{}^j \le t \le b_o{}^j$. In addition, equations (2.37) through (2.40) hold on E_o.

(c.) Inequality (2.41) holds for all points $x_o{}^j(t), u^j, t$ in $R_o{}^j$, $j = 1, \ldots, m$.

For the problem considered above each branch possesses the same number of state variables, an equal number of inequality constraints, etc. However, Theorem 1 and its corollary would remain essentially unchanged if the state vector or control vector or the ϕ^j vector functions had different dimensions on each branch. This flexibility permits an efficient model to be used for problems having branches of varying degrees of complexity.

BOUNDED STATE. In the previous definition of branched trajectories only those algebraic side conditions, ϕ, which contained the control explicitly were permitted. The case of pure state bounds is somewhat different in character and therefore will be given special attention here. The problem formulation and derivation of necessary conditions is sufficiently close to that required for the bounded state case so only the differences will be pointed out.

First, in the problem statement the region R_o^j is modified to include only the set of elements (x^j,u^j,t) such that (see Figure 4)

$$\phi_\alpha^j[x^j,t] \le 0 \qquad \begin{matrix}\alpha = 1,\ldots,s \\ j = 1,\ldots,m \\ a^j \le t \le b^j.\end{matrix} \tag{2.42}$$

A state-bounded branch, $\bar{E}^j$, is defined as the pair of parameters

$$a^j, b^j$$

and vector functions

$$x^j(t),\ u^j(t)$$

satisfying differential equations (2.1) and relations (2.42).

With this definition of $\bar{E}^j$ a state-bounded branched trajectory, $\bar{E}$, is defined as a set of m state-bounded branches which satisfy the boundary conditions (2.6).

Among all possible state-bounded branched trajectories, $\bar{E}$, one which minimizes the performance index (2.7) is called a minimal state-bounded branched trajectory and denoted by $\bar{E}_o$.

Once again the linear transformation (2.8) is applied on each branch mapping each branch on the interval $o \le T \le 1$. Each part of the problem transforms as before except that, since equations (2.2-3) have been replaced by (2.42), the expressions (2.10-11) must be replaced by

$$\psi_\alpha^j[y^j,a^j,b^j,T] \le 0 \qquad \begin{matrix} j = 1,\ldots,m \\ \alpha = 1,\ldots,s.\end{matrix} \tag{2.43}$$

The transformed problem is now a conventional (single-branch), fixed interval ($o \le T \le 1$) optimal control problem with bounded state. Necessary conditions for a very similar problem are given by Hestenes (ref. 13, page 354). The following is a modification of Hestenes' results (the modification merely accounts for the variable terminal states).

To account for the effect of the state bounds on the variations of the end points of the trajectory the following additional boundary conditions must be introduced.

$$g_{p+(j-1)s+\alpha} = \psi_\alpha^j[y^j(o),a^j(o),b^j(o),o] + (\gamma_\alpha^j)^2 = 0 \tag{2.44}$$

$$g_{p+ms+(j-1)s+\alpha} = \psi_\alpha^j[y^j(1),a^j(1),b^j(1),1] + (\beta_\alpha^j)^2 = 0. \tag{2.45}$$

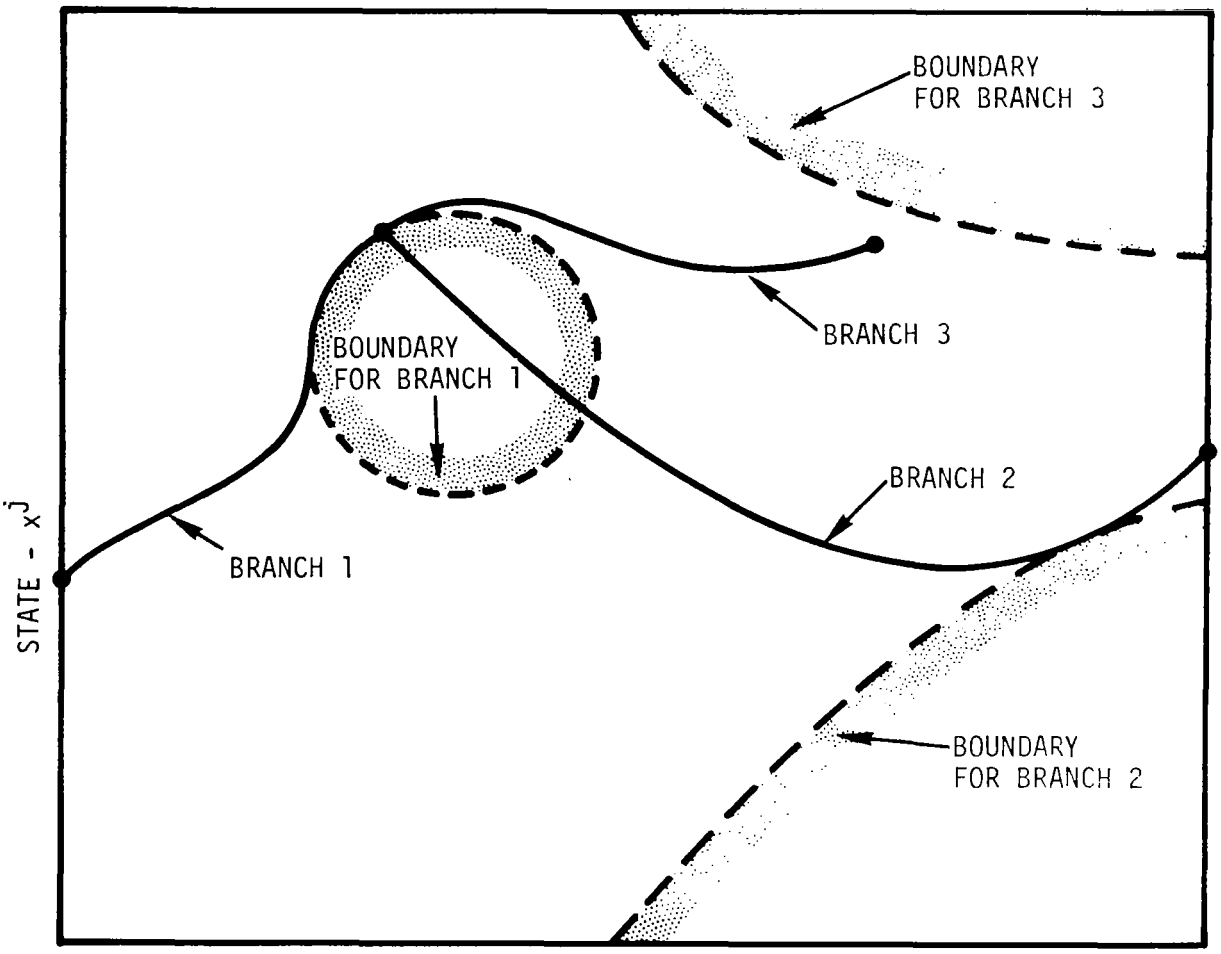

Note: Branch 1 terminates on its boundary; branch 2 begins on branch 1 boundary, passes through the branch 1 restricted zone, intersects and leaves the branch 2 boundary; branch 3 starts on the branch 1 boundary and never encounters the branch 3 boundary.

Figure 4. Branched Trajectory with State Bounds

Theorem 2. Let $\bar{E}_o^*$, with components $Z_o(T), U_o(T)$, be a minimal trajectory for the transformed problem just described. There exist multipliers $\lambda_o \geq 0$ and

$$\Lambda_i^j(T), \Gamma_j^a(T), \Gamma_j^b(T), M_\alpha^j(T), \varepsilon_e$$

$$(j=1,\ldots,m; \quad i=1,\ldots,n; \quad \alpha=1,\ldots,s \; ; \; e=1,\ldots,p+2ms)$$

and functions

$$K^j[y^j,a^j,b^j,v^j,\Lambda^j,M^j,T] = \Lambda^j \cdot h^j - \lambda_o \dot{h}_o{}^j - M^j \cdot \psi^j \tag{2.46}$$

$$K[Z,v,\Lambda,M,T] = \sum_{j=1}^{m} (b^j - a^j) K^j \tag{2.47}$$

and

$$F[Z(o),Z(1)] = \lambda_o g_o[y(o),y(1),a(o),b(o)] + \varepsilon \cdot g[y(o),y(1),a(o),b(o)] \tag{2.48}$$

such that

(i) The multipliers $M^j(T)$ are piecewise continuous and the multipliers

$$\Lambda(T), \Gamma^a(T), \Gamma^b(T)$$

are continuous and have piecewise continuous derivatives on $0 \leq T \leq 1$ and satisfy with

$$Z_o(T), \; v_o(T)$$

the Euler-Lagrange equations (2.19-26) on each interval of continuity of $v_o{}^j(T)$. The functions

$$K^j[y_o{}^j(T),a_o{}^j(T),b_o{}^j(T),\Lambda^j(T),M^j(T),T]$$

are continuous on $0 \leq T \leq 1$ and the transversality condition (2.27) holds on $\bar{E}_o^*$ for all $dz(o), dz(1), d\gamma$ and $d\beta$.

(ii) The inequality (2.49) holds for all $(z_o(T),v,T)$ in S_o where S_o is defined by relations (2.43).

$$K[Z_o(T),v,\Lambda(T),M(T),T] \leq K[Z_o(T),v_o(T),\Lambda(T),M(T),T] \tag{2.49}$$

(iii) For each pair of indicies α,j the multiplier

$$M_\alpha^j(T) \qquad 0 \leq T \leq 1$$

is nonincreasing and is constant on every interval on which

(2.50) $$\rho_\alpha^j(T) = \psi_\alpha^j[y_o^j(T),\ a_o^j(T),\ b_o^j(T),\ T] < 0.$$

It is continuous whenever $v_o^j(T)$ is continuous and at every point at which

$$\frac{d}{dT}\left[\rho_\alpha{}^j(T)\right]$$

is discontinuous.

(iv) At no point T on $0 \le T \le 1$ are the multipliers

$$\lambda_o, \Lambda(T), \Gamma^{\,a}(T), \Gamma^{\,b}(T)$$

of the form

$$\lambda_o = 0$$

$$\Lambda(T) = C \cdot \psi_y[y_o, a_o, b_o, T]$$

$$\Gamma^{\,a}(T) = C \cdot \psi_a[y_o, a_o, b_o, T]$$

$$\Gamma^{\,b}(T) = C \cdot \psi_b[y_o, a_o, b_o, T]$$

where C is any ms-dimensional constant vector.

The process of inverting the transformation is the same as before and will not be repeated here. Instead only the resulting necessary conditions will be given.

Theroem 2-A. Let $\bar{E}_o$ be a minimal state-bounded branched trajectory. There exist multipliers $\lambda_o \ge 0$ and

$$\lambda_i^j(t),\ \mu_\alpha^j(t),\ \varepsilon_e$$

$$(j = 1,\ldots,m;\ i = 1,\ldots,n;\ \alpha = 1,\ldots,s;\ e = 1,\ldots,p+2ms)$$

and functions (2.29) and (2.30) such that on $a^j \le t \le b^j$ for $j=1,\ldots,m$

(a) The multipliers $\lambda^j(t)$ are continuous and satisfy with $x_o^j(t)$, $u_o^j(t)$ the equations

(2.51) $$\dot{x}^j = H^j_{\lambda^j}$$

(2.52) $$\dot{\lambda}^j = -\,H^j_{x^j}$$

(2.53) $$H^j_{u^j} = 0$$

(2.54) $$\dot{H}^j = H_t^j$$

on each interval of continuity of $u_o^j(t)$. The functions

$$H^j[x_o^j(t),\ u_o^j(t),\ \lambda^j(t),\ \mu^j(t),t]$$

are continuous. The equations

(2.55) $$\frac{\partial G}{\partial a^j} + H^j(a^j) = 0$$

(2.56) $$\frac{\partial G}{\partial b^j} - H^j(b^j) = 0$$

(2.57) $$\frac{\partial G}{\partial x^j(a^j)} - \lambda^j(a^j) = 0$$

(2.58) $$\frac{\partial G}{\partial x^j(b^j)} + \lambda^j(b^j) = 0$$

are satisfied along with

(2.59) $$\varepsilon_{p+(j-1)s+\alpha}\,\gamma_\alpha^j = 0$$

(2.60) $$\varepsilon_{p+ms+(j-1)s+\alpha}\,\beta_\alpha^j = 0.$$

(b) The inequality

$$H^j[x_o^j(t),u^j,\lambda^j(t),\mu^j(t),t] \le H^j[x_o^j(t),u_o^j(t),\lambda^j(t),\mu^j(t),t]$$

holds for all u^j such that $(x_o^j(t),u^j,t)$ is in R_o^j.

(c) For each index α, the multiplier $\mu_\alpha^j(t)$ is nonincreasing and is constant on every interval on which

$$\phi_\alpha^j[x_o^j(t),t] < 0.$$

It is continuous where $u_o^j(t)$ is continuous and at every point at which

$$\frac{d}{dt}[\phi_\alpha^j]$$

is discontinuous.

(d) At no point t are the multipliers $\lambda_o,\lambda^j(t)$ of the form

$$\lambda_o = 0$$

$$\lambda^j = d \cdot \oint_{x^j}^{j} [x_o^j(t),t]$$

where d is any s-dimensional constant vector.

It should be noted that the transversality equations of Theorem 2-A differ from those of Theorem 1-A because of the difference in the definitions of G. For Theorem 1-A

$$G \equiv \lambda_o g_o + \sum_{e=1}^{p} \varepsilon_e g_e$$

but for Theorem 2-A

$$G \equiv \lambda_o g_o + \sum_{e=1}^{p+2ms} \varepsilon_e g_e$$

where the last (2ms) of the functions, g_e, are defined by (2.44-45).

3.0 SOME GEOMETRIC EXAMPLES

In order to become familiar with a new technique it is usually helpful to try that technique on a simple problem which has already been solved. Unfortunately, most aerospace applications are so complex that they cannot be solved in closed form. For that reason two non-aerospace problems, basically geometric in nature, have been chosen to display the branched trajectory concept.

As mentioned earlier the first example of an optimal branched trajectory was probably given by Mary Sinclair (ref. 4) in 1909. Rather than developing a general format for branched trajectories, Miss Sinclair directly examined a soap bubble problem which happens to fall under the category of branched trajectories.

The more familiar soap bubble problem is that of finding a curve connecting two given points in the x-y plane and on the same side of the y-axis such that the surface of revolution of the curve about the y-axis is a minimum. The resulting solution shown in Figure 5 is a catenary connecting the given points A_o, A_1. It has been observed that soap bubbles under certain circumstances indeed do assume the shape of a catenary of revolution. The solution to this problem may be obtained with conventional optimal control techniques.

Miss Sinclair's soap bubble differs slightly from the form just described. It may be described as a surface of revolution generated by rotating three curves (labeled branches 1, 2 and 3 in Figure 6) about a given axis. These three curves as shown in Figure 6 are joined at point A_2. One curve terminates at the y-axis and one each at the given points A_o, A_1. The points A_o and the coordinate Y_o are free. The optimization problem is that of determining the three curves described above such that the surface of revolution generated by rotating these curves about the y-axis is a minimum.

In control (and branch) notation the problem can be stated as follows:

$$(3.1) \qquad \text{Minimize} \qquad J = \sum_{j=1}^{3} \int_{a^j}^{b^j} x \sec u^j \, dx$$

(where J is the area of the surface of revolution divided by 2π)

subject to the differential equation

$$(3.2) \qquad \frac{dy^j}{dx} = \tan u^j \qquad\qquad j = 1,2,3$$

and the boundary conditions

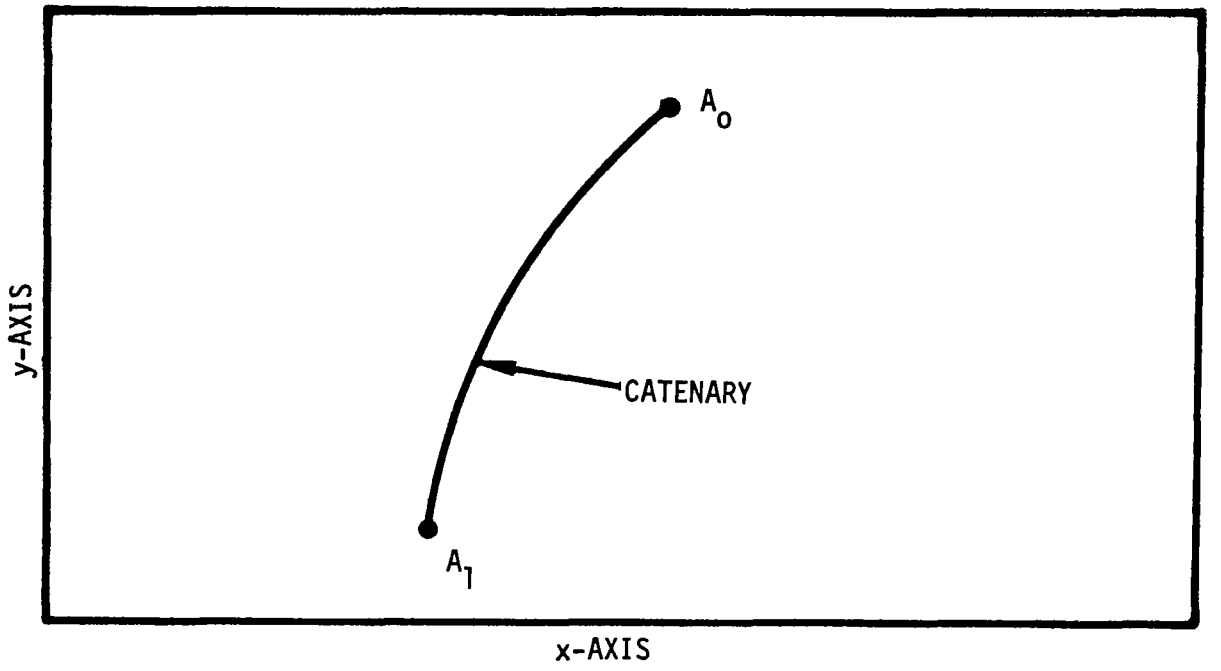

Figure 5. Single Arc Soap Bubble Problem

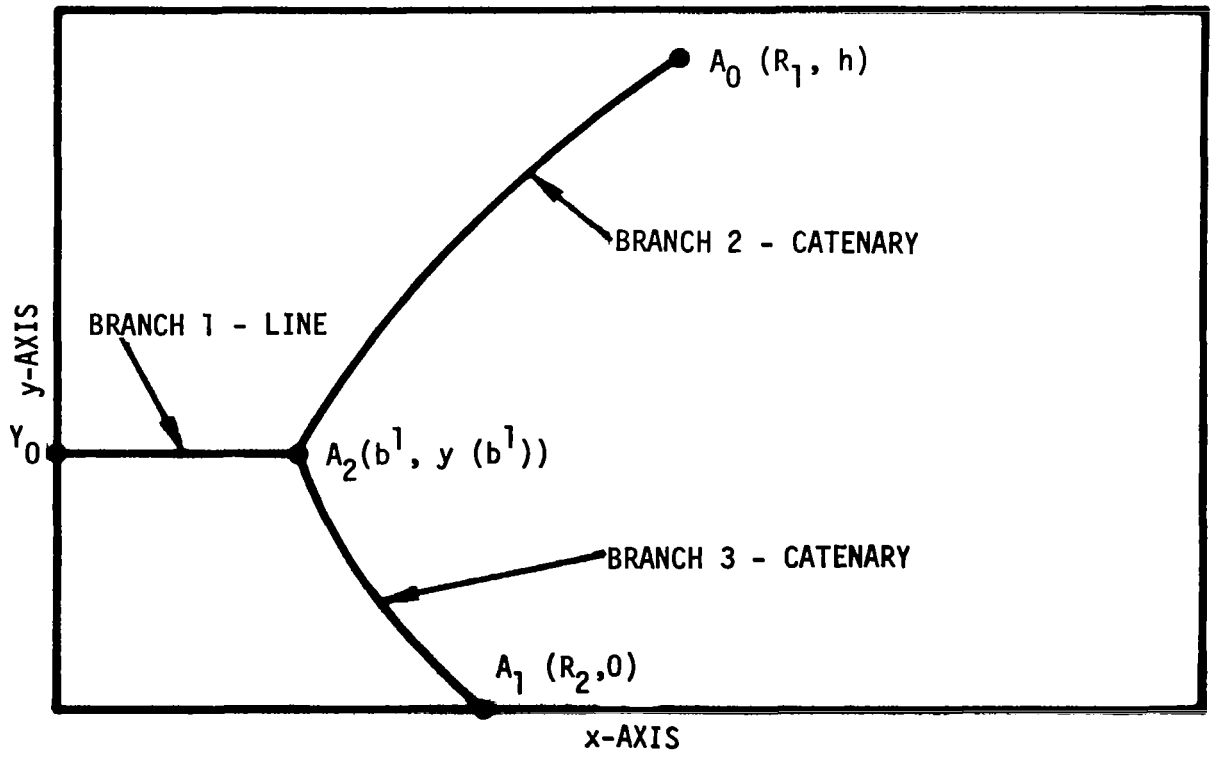

Figure 6. Branched Soap Bubble Problem

(3.3) $g_1 = a^1 = 0$

(3.4) $g_2 = a^2 - b^1 = 0$

(3.5) $g_3 = y(a^2) - y(b^1) = 0$

(3.6) $g_4 = a^3 - b^1 = 0$

(3.7) $g_5 = y(a^3) - y(b^1) = 0$

(3.8) $g_6 = b^2 - R_1 = 0$

(3.9) $g_7 = y(b^2) - h = 0$

(3.10) $g_8 = b^3 - R_2 = 0$

(3.11) $g_9 = y(b^3) = 0.$

On the j-th branch the variational Hamiltonian as defined by (2.29) is

(3.12) $H^j \equiv \lambda^j \tan u^j - x \sec u^j$

so the Euler-Lagrange equations (eqn. 2.32-33) are

(3.13) $\dot{\lambda}^j = 0$

and

(3.14) $\lambda^j \sec^2 u^j - x \sec u^j \tan u^j = 0.$

The first of these equations implies that λ^j = constant for j = 1, 2,3. Since the secant function is never zero the control equation implies

(3.15) $\lambda^j = x \sin u^j \qquad j = 1,2,3.$

Making this substitution in (3.12) yields

(3.16) $H^j \equiv - x \cos u^j \qquad j = 1,2,3.$

Because $g_9 \equiv 0$ for this problem the function G as defined by equation (2.30) is

(3.17) $G \equiv \sum_{e=1}^{9} \varepsilon_e g_e$

and transversality conditions (2.37-40) are for j=1 :

$$\varepsilon_1 + H^1(a^1) = 0$$
$$-\varepsilon_2 - \varepsilon_4 - H^1(b^1) = 0$$
$$- \lambda^1(a^1) = 0$$
$$-\varepsilon_3 - \varepsilon_5 + \lambda^1(b^1) = 0$$

for j = 2 :

$$\varepsilon_2 + H^2(a^2) = 0$$
$$\varepsilon_6 - H^2(b^2) = 0$$
$$\varepsilon_3 - \lambda^2(b^2) = 0$$
$$\varepsilon_7 + \lambda^2(b^2) = 0$$

for j = 3 :

$$\varepsilon_4 + H^3(a^3) = 0$$
$$\varepsilon_8 - H^3(b^3) = 0$$
$$\varepsilon_5 - \lambda^3(a^3) = 0$$
$$\varepsilon_9 + \lambda^3(b^3) = 0$$

Since there are 12 of these equations and only 9 of the multipliers, ε, that leaves 3 independent conditions. These may be obtained by eliminating all of the ε's.

(3.18) $$\lambda^1(a^1) = 0$$

(3.19) $$\lambda^1(b^1) = \lambda^2(a^2) + \lambda^3(a^3)$$

(3.20) $$H^1(b^1) = H^2(a^2) + H^3(a^3)$$

Equations (3.13) and (3.14), for j = 1, together with (3.18) imply that

(3.21) $$\lambda^1(t) \equiv 0$$

(3.22) $$u^1(t) \equiv 0$$

So branch 1 is a line segment parallel to the x axis and

$$y^1(t) \equiv y^1(a^1) = Y_o. \tag{3.23}$$

Now, equation (3.19) indicates that

$$-\lambda^3(t) \equiv \lambda^2(t) \tag{3.24}$$

and

$$u^3(a^3) = - u^2(a^2). \tag{3.25}$$

Equation (3.20) may be written as

$$-b^1 \cos u^1(b^1) = -a^2 \cos u^2(a^2) - a^3 \cos u^3(a^3) \tag{3.26}$$

Combining (3.22), (3.25) and (3.26) and using the boundary conditions (3.4) and (3.6)

$$1 = 2 \cos u^2(a^2)$$

or

$$u^2(a^2) = 60^\circ \tag{3.27}$$

and

$$u^3(a^3) = -60^\circ. \tag{3.28}$$

From (3.15)

$$\lambda^2(t) \equiv \frac{\sqrt{3}}{2} b^1 \tag{3.29}$$

and

$$\lambda^3(t) \equiv -\frac{\sqrt{3}}{2} b^1. \tag{3.30}$$

Let $C = \frac{\sqrt{3}}{2} b^1$ so that

$$\tan u^2(t) = \frac{C}{\sqrt{x^2-C^2}} \tag{3.31}$$

and

$$\tan u^3(t) = \frac{-C}{\sqrt{x^2-C^2}} \tag{3.32}$$

Integrating (3.2), for $j = 2,3$, and using the appropriate boundary values leads to the final solution which has been simplified for the case $R_1 = R_2 = R$.

$$(3.33) \qquad y^1(x) \equiv \frac{h}{2} \qquad 0 \le x \le \frac{2}{\sqrt{3}} C$$

$$(3.34) \qquad y^2(x) \equiv \frac{h}{2} - C \log(\sqrt{3}) + C \left/ \cosh^{-1}\left(\frac{x}{C}\right)\right. \qquad \frac{2}{\sqrt{3}} C \le x \le R$$

$$(3.35) \qquad y^3(x) \equiv \frac{h}{2} + C \log(\sqrt{3}) - C \left/ \cosh^{-1}\left(\frac{x}{C}\right)\right. \qquad \frac{2}{\sqrt{3}} C \le x \le R$$

where C satisfies

$$(3.36) \qquad \frac{R}{C} = \cosh\left[\frac{h}{2C} + \log(\sqrt{3})\right].$$

The solution of the branched soap bubble problem consists of a line segment for branch 1 and a catenary for each of branches 2 and 3. Apparently, none of the branches degenerate to zero length as the parameters h and R take on increasing positive values. However, Sinclair (ref.4) shows that the three branch solution is not stable if any branch contains a conjugate point (i.e., fails to satisfy Jacobi's necessary condition).

A MINIMUM DISTANCE PROBLEM. A very simple example which demonstrates some of the short comings of the theory is that of finding the shortest path consisting of three branches and connecting three points as shown in Figure 7. Without loss of generality one point may be placed at the origin, one on the positive x-axis a unit distance from the origin and a third at a general point (h,k) in the first quadrant.

The state x_1^j, x_2^j on the j-th branch evolves according to the differential equations

$$(3.37) \qquad \frac{dx_1^j}{ds} = \cos u^j$$

$$(3.38) \qquad \frac{dx_2^j}{ds} = \sin u^j \qquad j = 1,2,3$$

where the control u^j is the slope of the path in $x_1 - x_2$ space.

The performance criterion is just the sum of the lengths of the three branches.

$$(3.39) \qquad J \equiv \sum_{j=1}^{3} \int_{a^j}^{b^j} ds$$

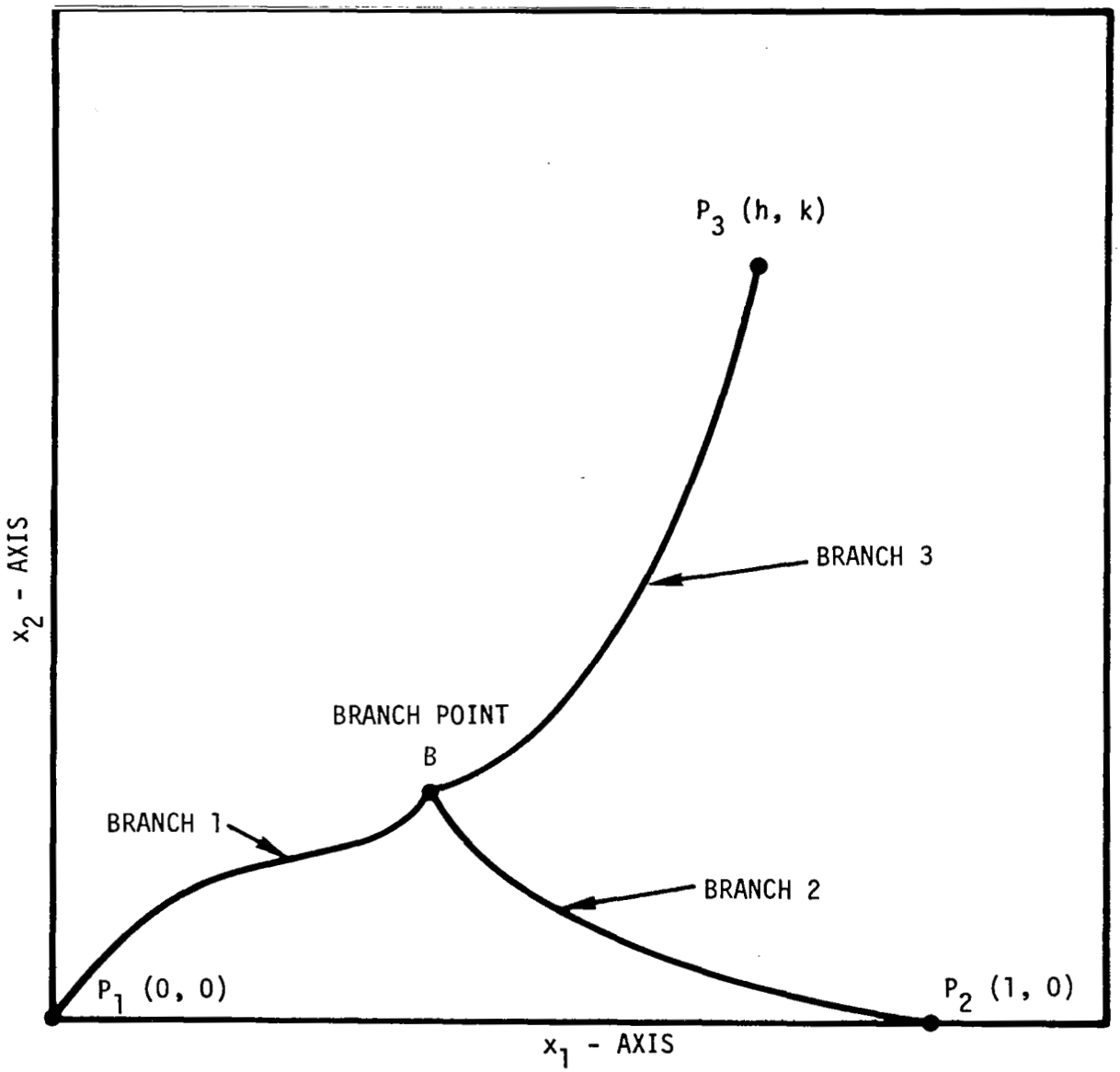

Figure 7. Three Point Minimum Distance Problem

Using the branch numbering from figure 7, the boundary conditions are:

$$g_1 = a^1 = 0 \qquad g_8 = x_1(b^3) - h = 0$$

$$g_2 = a^2 = 0 \qquad g_9 = x_2(b^3) - k = 0$$

$$g_3 = a^3 = 0 \qquad g_{10} = x_1(a^2) - x_1(b^1) = 0$$

$$g_4 = x_1(a^1) = 0 \qquad g_{11} = x_2(a^2) - x_2(b^1) = 0$$

$$g_5 = x_2(a^1) = 0 \qquad g_{12} = x_1(a^3) - x_1(b^1) = 0$$

$$g_6 = x_1(b^2) - 1 = 0 \qquad g_{13} = x_2(a^3) - x_2(b^1) = 0$$

$$g_7 = x_2(b^2) = 0$$

This completes the problem statement. The H function on each subarc is

$$H^j = \lambda_1^j \cos u^j + \lambda_2^j \sin u^j - 1 \qquad j = 1,2,3 \tag{3.40}$$

Applying the Euler-Lagrange equations determines that λ_1^j and λ_2^j are constant, $j = 1,2,3$, and that

$$\tan u^j = \frac{\lambda_2^j}{\lambda_1^j} \qquad j = 1,2,3. \tag{3.41}$$

Applying equations (2.38) shows that

$$H^j(b^j) = 0 \qquad j = 1,2,3. \tag{3.42}$$

The remaining transversality conditions eventually lead to the result

$$\lambda_1^1 = \lambda_1^2 + \lambda_1^3 \tag{3.43}$$

and

$$\lambda_2^1 = \lambda_2^2 + \lambda_2^3. \tag{3.44}$$

Equation (3.42) along with (2.34) imply that

$$\lambda_1^j \cos u^j + \lambda_2^j \sin u^j = 1. \tag{3.45}$$

This together with equation (3.41) permit the following result.

(3.46) $\lambda_1^j = \cos u^j$

(3.47) $\lambda_2^j = \sin u^j$.

Since λ_1^j and λ_2^j are constant the slope u^j is constant and each branch is a line segment. It only remains to discover at what angles these lines intersect. Equations (3.43-47) indicate that

$$\cos u^1 = \cos u^2 + \cos u^3$$

$$\sin u^1 = \sin u^2 + \sin u^3.$$

These equations are satisfied by

$$u^2 = u^1 - 60^\circ$$

and

$$u^3 = u^1 + 60^\circ.$$

That means that the three branches must intersect at 120° with respect to each other. Point B, the branch point must be located such that line segments connecting point B with each of the points P_1, P_2 and P_3 intersect at 120°. Obviously, there exist some locations of point P_3 such that no proper branch point may be chosen (for example, take $k^3 = 1$ and $h = 100$). In these instances, there are no solutions having three branches. Instead a two branch solution must be used. This type of degeneracy, represents a real obstacle to the numerical solution of complex branched trajectory problems. If "physical insight" does not dictate the correct number of branches, considerable time could be wasted in attempting to obtain a solution which does not exist.

Figure 8 shows the locus of branch points for $k = 1$ and h increasing from 1/2 to $(1 + \sqrt{3}/3)$. As h approaches the value $(1 + \sqrt{3}/3)$ the branch point approaches P_2 and the second branch degenerates to zero length. At this point the analysis falls apart and for greater value of h a three branch solution does not exist. Of course one may still look for two branch solutions.

The procedure used above was to apply Theorem 1-A directly to the original problem formulation. It was not necessary to transform the original problem because Theorem 1-A is stated in terms of branched trajectories. However, the alternate procedure of transforming the original problem to the format of conventional optimal control and solving that problem by applying Theorem 1 may be both instructional and practical for some numerical schemes. This latter approach is briefly sketched below for the previous minimum distance example.

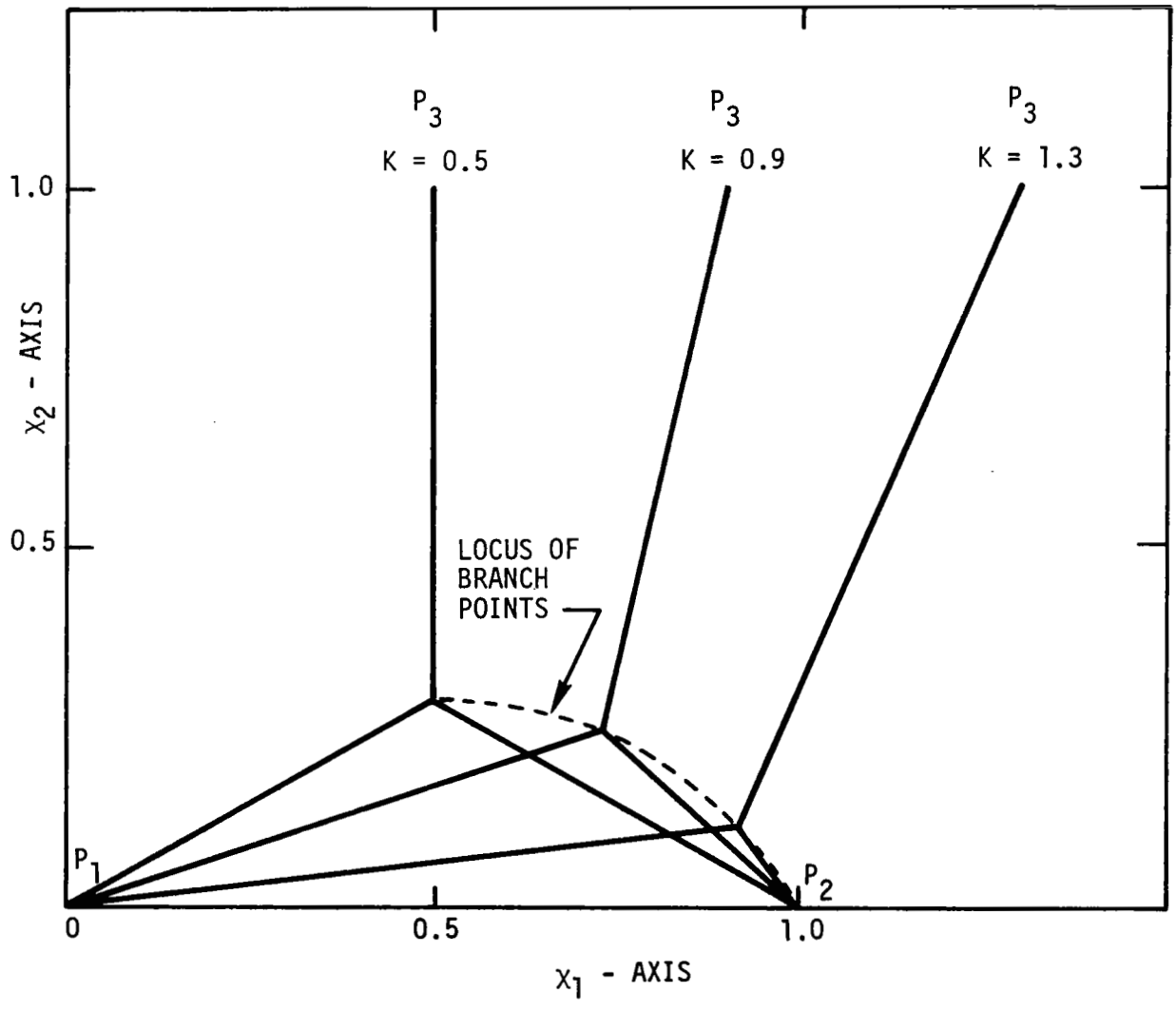

Figure 8. Locus of Branch Points

On each of the three branches replace S as the independent variable by T according to the relation

$$S = a^j + (b^j - a^j)T \qquad 0 \le T \le 1, \quad j = 1,2,3 \tag{3.48}$$

Now, following the same notation used in section 2, equations (3.37-3.38) become

$$\frac{dy_1^j}{dT} = (b^j - a^j)\cos v^j \tag{3.49}$$

$$\frac{dy_2^j}{dT} = (b^j - a^j)\sin v^j \qquad j = 1,2,3, \quad 0 \le T \le 1 \tag{3.50}$$

The performance criterion (3.39) transforms into

$$I \equiv \sum_{j=1}^{3} \int_0^1 (b^j - a^j)dT \tag{3.51}$$

Since the a^j's and b^j's will be treated as state variables, six additional differential equations must be included.

$$\frac{da^j}{dT} = 0 \tag{3.52}$$

$$\frac{db^j}{dT} = 0 \qquad j = 1,2,3, \quad 0 \le T \le 1 \tag{3.53}$$

The boundary conditions g_1 through g_{13} remain unchanged except for replacing a^j by $a^j(0)$ in g_1, g_2, and g_3. The variational Hamiltonian for the transformed problem is given by (2.17).

$$K \equiv \sum_{j=1}^{3} (b^j - a^j)K^j \tag{3.54}$$

where $$K^j \equiv \Lambda_1^j \cos v^j + \Lambda_2^j \sin v^j - \lambda_o$$

Application of the necessary conditions of Theorem 1 to this formulation results in the same solution as that obtained by using Theorem 1-A directly. This example was also discussed by Mason (ref. 14).

4.0 AEROSPACE APPLICATIONS

In order to evaluate the utility of optimal branched trajectories with respect to trajectory design and guidance development, five areas were examined. These are: (1) the trajectory design for multiple payload launch vehicles; (2) the inclusion of optimal staging techniques in the foregoing example; (3) the trajectory design for secondary or abort, mission optimization; (4) branching lander/orbiter type space maneuvers such as those available to the lunar module (LM) and control-service module (CSM) of the Apollo project; and (5) air traffic terminal control. Some numerical results were obtained for problems (1), (3) and (4); this data is presented in section 5.0.

MULTIPLE PAYLOAD LAUNCHES. The mission profiles for this example are sketched in Figure 9. Two payloads are to be inserted into two separate orbits. In the conventional approach (represented by the dashed line in Figure 9) two optimal trajectories are computed separately, the first starting at the initial point and ending at the required orbit for payload number 1 and the second starting in that orbit and proceeding to payload number 2's orbit. In the branched case the vehicle separates into two parts prior to reaching the first orbit.

The equations of motion to be used for this example include only the effects of inverse square gravity in two dimensions.

$$\dot{v} = \frac{T}{m} \cos \theta - \frac{\mu}{r^2} \sin \gamma \tag{4.1}$$

$$\dot{\gamma} = \frac{T}{mv} \sin \theta - \left(\frac{\mu}{r^2 v} - \frac{v}{r} \right) \cos \gamma \tag{4.2}$$

$$\dot{r} = v \sin \gamma \tag{4.3}$$

$$\dot{\phi} = \frac{v}{r} \cos \gamma \tag{4.4}$$

$$\dot{m} = - \beta \tag{4.5}$$

The state variables v, γ, r, ϕ and m are defined as the modulus of velocity, the flight path angle referenced to the local horizontal, the radial distance from the central body, the range angle and the mass respectively. The control variable θ is the angle of attack (or the angle between the velocity and thrust vectors). The remaining parameters, T, β and μ, are the thrust magnitude, mass flow rate and the gravitational parameter. Superscripts indicating branch number will not be used since the same equations, except for parametric changes, apply to each branch and little possibility for confusion will arise.

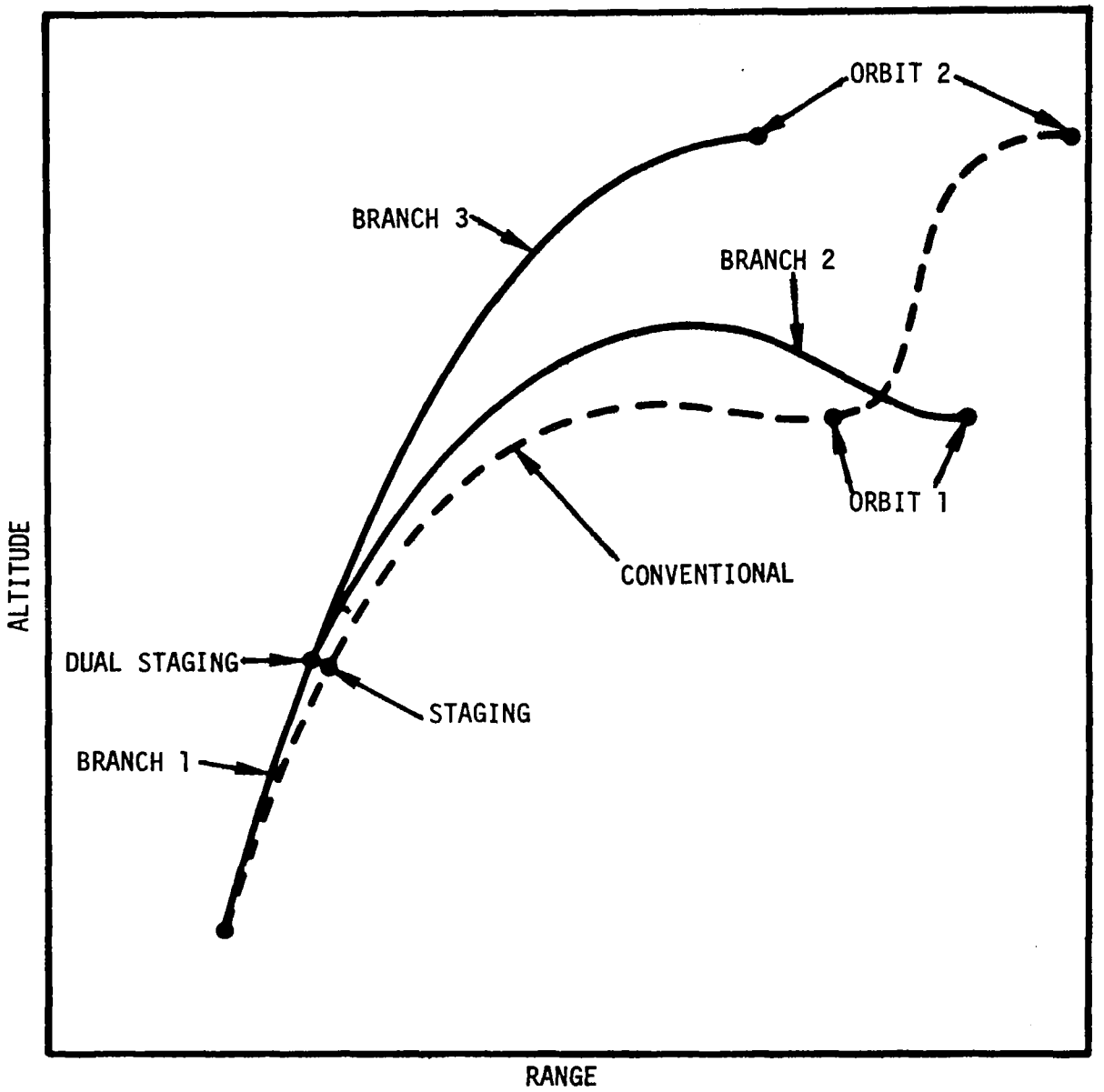

Figure 9. Mission Profile for Two Payload Launch

Although some of the problem boundary conditions are quite obvious and can be applied trivially, the complete set will be stated. The boundary conditions defining the fixed initial state and time of branch 1 are

$$g_1 = a^1 = 0$$

$$g_2 = v(a^1) - v_1 = 0$$

$$g_3 = \gamma(a^1) - \gamma_1 = 0$$

$$g_4 = r(a^1) - r_1 = 0$$

$$g_5 = \phi(a^1) - \phi_1 = 0$$

$$g_6 = m(a^1) - m_1 = 0.$$

Branch 2 is "attached" to the end of branch 1 by equating appropriate variables.

$$g_7 = a^2 - b^1 = 0$$

$$g_8 = v(a^2) - v(b^1) = 0$$

$$g_9 = \gamma(a^2) - \gamma(b^1) = 0$$

$$g_{10} = r(a^2) - r(b^1) = 0$$

$$g_{11} = \phi(a^2) - \phi(b^1) = 0$$

$$g_{12} = m(a^3) + m(a^2) - m(b^1) + \Delta m_1 = 0$$

where Δm_1 is the specified structural mass of the first stage. Similarly, branch 3 is attached to branch 1

$$g_{13} = a^3 - b^1 = 0$$

$$g_{14} = v(a^3) - v(b^1) = 0$$

$$g_{15} = \gamma(a^3) - \gamma(b^1) = 0$$

$$g_{16} = r(a^3) - r(b^1) = 0$$

$$g_{17} = \phi(a^3) - \phi(b^1) = 0$$

Also, the burn time for branch 1 is fixed,

$$g_{18} = b^1 - t_1 = 0$$

and the initial mass for branch 2 is specified

$$g_{19} = m(a^2) - m_o = 0.$$

The orbit for payload number 1 must be defined by boundary conditions.

$$g_{20} = v(b^2) - v_2 = 0$$

$$g_{21} = \gamma(b^2) = 0$$

$$g_{22} = r(b^2) - r_2 = 0$$

$$g_{23} = m(b^2) - m_2 = 0$$

This last condition specifies the magnitude of payload number 1.

The remaining boundary conditions establish a circular orbit for payload number 2.

$$g_{24} = v(b^3) - v_3 = 0$$

$$g_{25} = \gamma(b^3) = 0$$

$$g_{26} = r(b^3) - r_3 = 0$$

With the first payload fixed the optimization is based on maximizing the second payload or for a minimization problem

$$J = g_o = -m(b^3).$$

Other formulations such as fixing both payloads and minimizing the lift off mass would be handled in a similar fashion.

Applying Theorem 1-A of section 2.0, the Euler-Lagrange equations for this problem are

(4.6) $$\dot{\lambda}_v = \lambda_\gamma\left[\frac{T}{mv^2}\sin\theta - \left(\frac{\mu}{r^2v^2} + \frac{1}{r}\right)\cos\gamma\right] - \lambda_r \sin\gamma - \lambda_\phi\left(\frac{1}{r}\cos\gamma\right)$$

(4.7) $$\dot{\lambda}_\gamma = \lambda_v \frac{\mu}{r^2}\cos\gamma + \lambda_\gamma\left[\frac{v}{r} - \frac{\mu}{r^2 v}\right]\sin\gamma - \lambda_r v\cos\gamma + \lambda_\phi\left(\frac{v}{r}\sin\gamma\right)$$

(4.8) $$\dot{\lambda}_r = -\lambda_v\left(\frac{2\mu}{r^3}\right)\sin\gamma + \lambda_\gamma\left[\frac{v}{r^2} - \frac{2\mu}{r^3 v}\right]\cos\gamma + \lambda_\phi\left(\frac{v}{r^2}\cos\gamma\right)$$

(4.9) $$\dot{\lambda}_\phi = 0$$

(4.10) $$\dot{\lambda}_m = \lambda_v\left(\frac{T}{m^2}\right)\cos\theta + \lambda_\gamma\left(\frac{T}{m^2 v}\right)\sin\theta$$

The control equation with the aid of the Weierstrass E test indicates that

(4.11) $$\sin\theta = \frac{\lambda_\gamma/v}{\lambda} \qquad \cos\theta = \frac{\lambda_v}{\lambda}$$

where

$$\lambda = \sqrt{\left(\frac{\lambda_\gamma}{v}\right)^2 + \lambda_v^2}\ .$$

Applying the transversality conditions as in the previous examples leads to several equations linear in the constant multipliers ε. Elimination of these multipliers yields the following results.

$$\lambda_v(a^2) + \lambda_v(a^3) = \lambda_v(b^1) \tag{4.12}$$

$$\lambda_\gamma(a^2) + \lambda_\gamma(a^3) = \lambda_\gamma(b^1) \tag{4.13}$$

$$\lambda_r(a^2) + \lambda_r(a^3) = \lambda_r(b^1) \tag{4.14}$$

$$\lambda_\phi(a^2) + \lambda_\phi(a^3) = \lambda_\phi(b^1) \tag{4.15}$$

$$\lambda_m(a^3) = \lambda_m(b^1) \tag{4.16}$$

$$\lambda_\phi(b^2) = 0 \tag{4.17}$$

$$H(b^2) = 0 \tag{4.18}$$

$$\lambda_\phi(b^3) = 0 \tag{4.19}$$

$$H(b^3) = 0 \tag{4.20}$$

$$\lambda_m(b^3) = 1 \tag{4.21}$$

Since equation (4.9) applies on all three branches then equations (4.17), (4.19) and (4.15) imply that

$$\lambda_\phi(t) = 0$$

on all three branches. Also since H is constant on all branches equations (4.18) and (4.20) indicate that $H(t) = 0$ on branches 2 and 3.

Stationary solutions are obtained by satisfying the Euler-Lagrange equations (4.6-8, 4.10) with the control given by (4.11) and meeting the terminal/corner conditions (4.12-14, 4.16, 4.21). Since (4.21) is the only equation which is not homogeneous with respect to the λ-multipliers it may be ignored allowing the remaining equations to be scaled by some constant. In other words the initial value of one of the multipliers may be set equal to unity.

If a Newton-Raphson iteration of unknown initial and branch point values (to satisfy terminal conditions) were used, then the order of the iteration would be five. The guesses might include, for example,

$$\lambda_\gamma(a^1), \lambda_r(a^1), \lambda_v(a^3), \lambda_\gamma(a^3), \lambda_r(a^3).$$

with

$$\lambda_v(a^1) = 1.$$

The first two guesses establish the control for the first branch and the second three the control for the third branch. Equations (4.12 -14) then yield the values of

$$\lambda_v(a^2), \lambda_\gamma(a^2), \lambda_r(a^2)$$

so the control for the second branch is also established.

For this two dimensional example there are five guesses. If the number of payloads (and therefore the number of branches) were increased to a total of P, then the number of guesses would be $2 + 3(P-1)$. So three new guesses are required for each additional payload.

OPTIMAL STAGING. The formulation of optimal branched trajectories may also be used to determine the optimal staging for the multiple payload. As in reference 8 let the structural mass for each stage be proportional to the burn time of that stage. Therefore, the structural mass to be discarded at the end of the j-th branch is

$$K_j(b^j - a^j) = \text{structural mass}$$

The formulation of the previous problem is unaltered except for boundary conditions 12,18,19,23 and the performance function. These become

$$g_{12} = m(a^3) + m(a^2) - m(b^1) + K_1(b^1 - a^1) = 0$$

$$g_{23} = m(b^2) - K_2(b^2 - a^2) - m_2 = 0$$

$$J = g_o = m(b^3) - K_3(b^3 - a^3).$$

The resulting transversality conditions are also the same as those of the previous example except that (4.18) and (4.20) are no longer valid and some additional conditions arise. These are

$$\lambda_m(a^2) = \lambda_m(b^1) \tag{4.22}$$

$$K_j\lambda_m(b^j) - H^j(b^j) = 0 \qquad j = 1,2,3 \tag{4.23}$$

Equations (4.23) are the switching functions which may be used to terminate the burning of each stage.

A Newton-Raphson iteration for this staging problem would involve seven guesses. In addition to those of the previous example it would be necessary to guess two additional values such as

$$\lambda_m(a^1) \text{ and } m(a^3).$$

Also for a P payload problem the number of guesses would be $3 + 4(P-1)$.

SECONDARY MISSION OPTIMIZATION. Complete mission planning must include a secondary or abort mission to be performed in the event the primary mission cannot be completed. When the launch vehicle capability exceeds that required for the primary mission, the excess propellant may be used to shape the primary mission trajectory so that the performance of a secondary mission is improved.

The secondary mission optimization problem can be stated most precisely with the aid of Figure 10. The trajectory is divided into three parts called branches. The first branch (arc OB) represents the path of the first stage of the vehicle. The arc BP represents the path of the last stage and point P is the orbit for the primary mission. If no failure occurs, the vehicle will travel along the path OBP. If the last stage has some malfunction at ignition or if, for some other reason, the primary mission is unobtainable at point B, the vehicle travels along arc BS with less than nominal thrust to achieve a secondary mission at S. As an example, in the Apollo mission if the S-IVB failed to ignite, service module propulsion could be used on arc BS. The particular point B is chosen as the most critical point of the trajectory (due to separation, ignition, etc.). Other critical points and their associated branches could be included as long as the number of branches is kept reasonably small. The arc OCP represents the usual optimal trajectory for the primary mission with no secondary considerations.

The trajectory optimization consists of jointly shaping the three branches such that the primary mission constraints at point P are satisfied and some performance criterion is extremized at point S. A specific orbit is chosen for the secondary mission and the final mass in this orbit is maximized. This procedure effectively maximizes the propellant remaining when the vehicle achieves the orbit. This propellant could then be used for further maneuvering.

Using Figure 10 as the basis for symbology, branch numbers 1 (OB), 2(BP) and 3(BS) are assigned to the vehicle configuration as follows:

Branch	Description
1	trajectory of the Saturn S-II class vehicle carrying the Saturn S-IVB, Lunar Excursion Module (LEM) and Command and Service Modules (CSM).
2	trajectory of the S-IVB carrying LEM and CSM
3	abort trajectory (from S-II burnout conditions) of the CSM (the loaded S-IVB and LEM are dropped for abort)

The equations of motion governing flight on each of the branches are identical to those of the previous examples (equations 4.1-5).

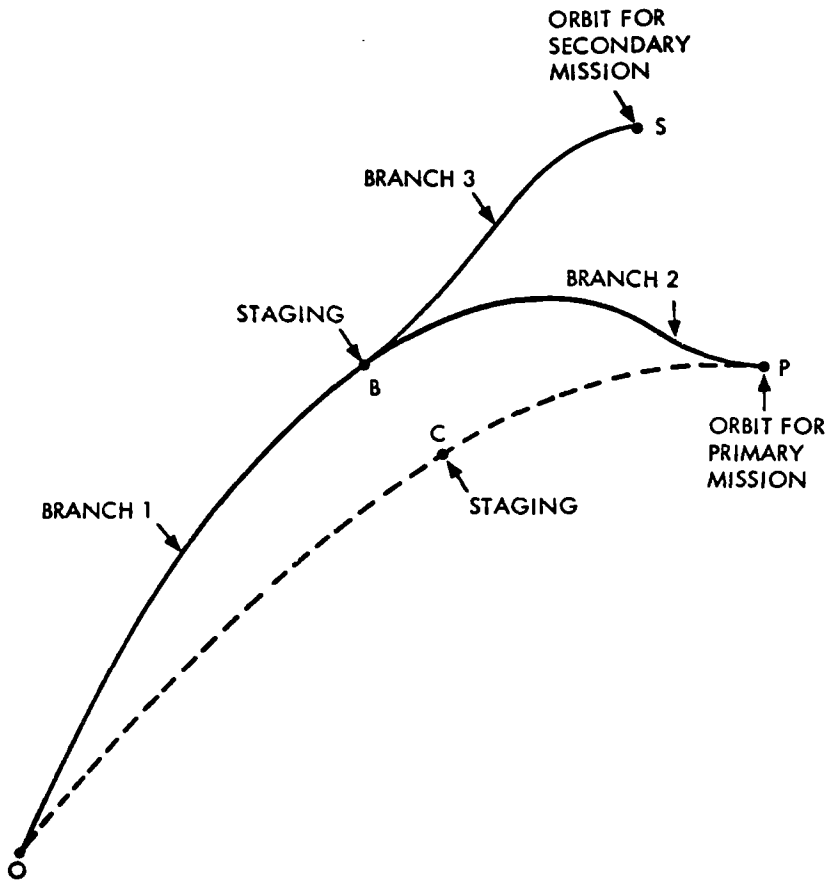

Figure 10. Mission Profile for Secondary Mission Consideration

The boundary conditions are also the same as those for the multiple payload case except for 19.

$$g_{19} = m(a^2) - m(b^1) + \Delta m_2 = 0$$

The resulting transversality conditions are given by equations (4.12-21) except that (4.16) becomes

$$\lambda_m(a^3) + \lambda_m(a^2) = \lambda_m(b^1). \tag{4.24}$$

Once again, five guesses are required in the numerical iteration procedure.

Some ground rules for choosing m_2, the primary payload, should be observed. First, it was assumed that there exists some required payload m_R which includes all necessary propellant reserves. With no branching (i.e. no secondary mission consideration) the vehicle can produce a maximum payload $m_0 > m_R$. This establishes an upper bound for m_2. It is also possible to establish a lower bound by computing an optimal (maximum payload) trajectory for the secondary mission with no consideration of the primary mission. That is, assume that failure will take place at the prescribed point and compute an optimal two-branch trajectory using branches 1 and 3 only. (Figure 10). Now with the branch point fixed compute an optimal branch 2 achieving a primary payload m_2. This procedure establishes a maximum secondary payload independent of m_2 and, therefore, a minimum practical value for m_2. Thus, in choosing m_2 impose the following bounds:

$$m_L < m_2 < m_0.$$

If

$$m_L < m_R < m_0$$

then let $m_2 = m_R$ and if $m_R < m_L$ let $m_2 = m_L$. Of course, if $m_R > m_0$ then the vehicle is incapable of accomplishing its primary mission.

LANDER/ORBITER MANEUVER. This application is similar mathematically to the multiple payload launch discussed earlier. In both cases the vehicle physically separates into two parts. The only real difference is in the set of terminal conditions.

As shown in Figure 11 the optimization problem begins at an arbitrary point on an approach hyperbola (point O). The spacecraft, which consists of two stages retro-thrusts to point B where the stages separate. After separation one stage descends to a landing configuration (point P) and the other stage proceeds to a circular parking orbit (point Q). On the descent maneuver, arc BP, a coasting arc CD is permitted.

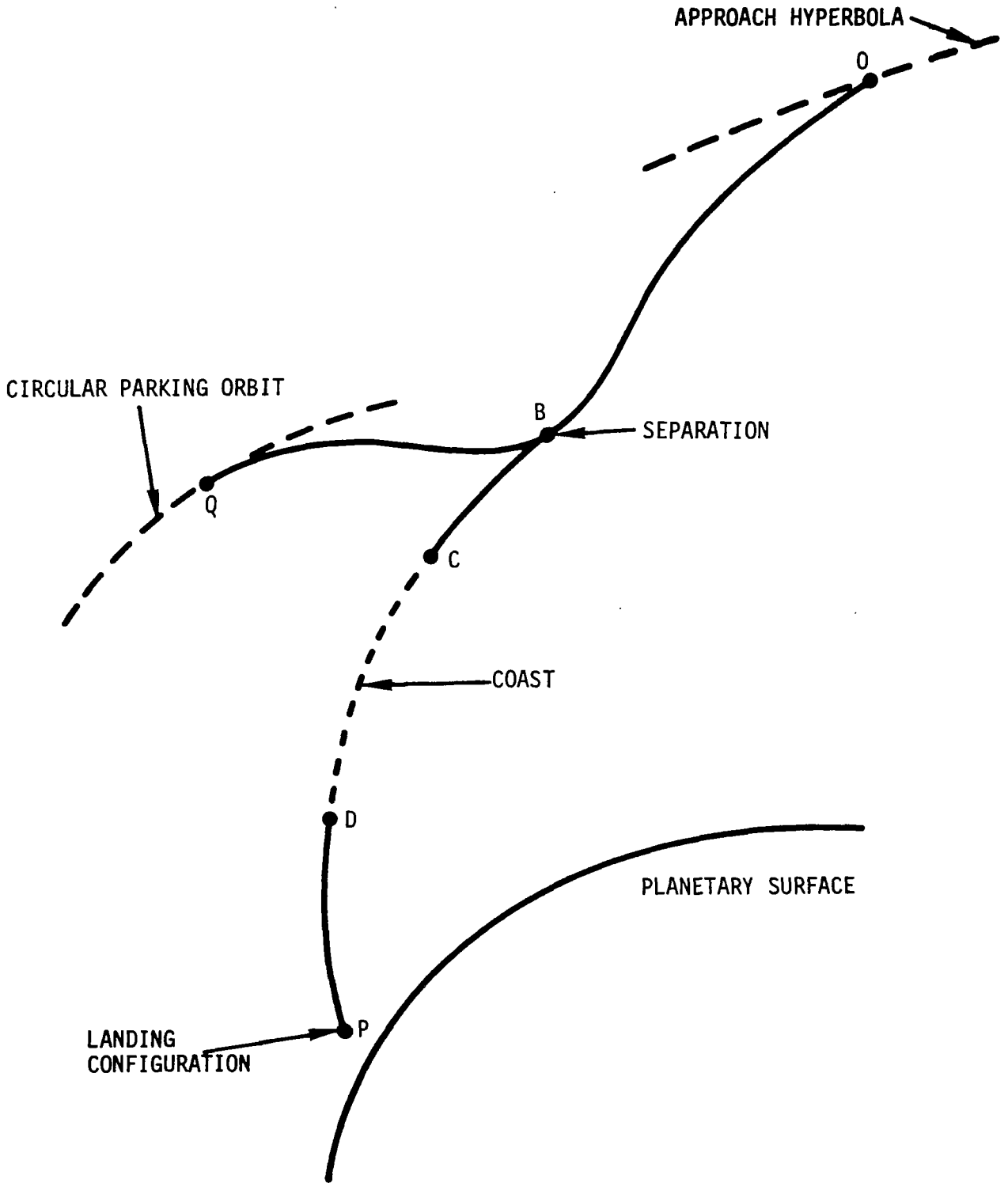

Figure 11. Mission Profile for Branched Lander/Orbiter Maneuver

Both the approach hyperbola and the parking orbit are fixed but the points of departure and entry are free. Also the velocity vector and altitude are specified for point P but the range is left free. The location and time of the branch point (B) are free as are the location and duration of the coasting arc CD.

It is desired to find a minimal branched trajectory of the type just described such that a fixed payload is inserted into the parking orbit and the payload placed in a landing configuration is maximized. Although the branch point (B) is free no staging will be performed. That is, the initial mass on the descent arc (BP) is prescribed.

Once again equations (4.1-5) will be used to represent the motion on each branch. With the branch numbering as given in Figure 11 the boundary conditions are as follows.

At the approach hyperbola:

$$g_1 = a^1 = 0$$

$$g_2 = 1/2\,[v(a^1)]^2 - \frac{\mu}{r(a^1)} - E_1 = 0$$

$$g_3 = r(a^1)\, v(a^1) \cos \gamma(a^1) - h_1 = 0$$

$$g_4 = \phi(a^1) = 0$$

$$g_5 = m(a^1) - M_1 = 0$$

At the branch point B:

$$g_6 = a^2 - b^1 = 0$$

$$g_7 = v(a^2) - v(b^1) = 0$$

$$g_8 = \gamma(a^2) - \gamma(b^1) = 0$$

$$g_9 = r(a^2) - r(b^1) = 0$$

$$g_{10} = \phi(a^2) - \phi(b^1) = 0$$

$$g_{11} = m(a^2) - M_2 = 0$$

$$g_{12} = a^3 - b^1 = 0$$

$$g_{13} = v(a^3) - v(b^1) = 0$$

$$g_{14} = \gamma(a^3) - \gamma(b^1) = 0$$

$$g_{15} = r(a^3) - r(b^1) = 0$$

$$g_{16} = \phi(a^3) - \phi(b^1) = 0$$

$$g_{17} = m(a^3) - m(b^1) + M_2 = 0$$

At point P:

$$g_{18} = v(b^2) - V_2 = 0$$

$$g_{19} = \gamma(b^2) - \gamma_2 = 0$$

$$g_{20} = r(b^2) - R_2 = 0$$

At the parking orbit, point Q:

$$g_{21} = v(b^3) - V_3 = 0$$

$$g_{22} = \gamma(b^3) = 0$$

$$g_{23} = r(b^3) - R_3 = 0$$

$$g_{24} = m(b^3) - M_3 = 0$$

The performance index is again

$$J = g_o = - m(b^2)$$

so that with these boundary conditions the associated transversality conditions become:

At point 0

$$H_o(a^1) = 0$$

where

$$(4.25) \qquad H_o(t) = - \lambda_v \frac{\mu}{r^2} \sin\gamma - \lambda_\gamma \left(\frac{\mu}{r^2 v} - \frac{v}{r}\right) \cos\gamma + \lambda_r v \sin\gamma$$

At the branch point equations (4.12-16) apply along with

$$(4.26) \qquad H^2(a^2) + H^3(a^3) = H^1(b^1).$$

The above equation may be reduced by observing that

$$H = L + H_o$$

where

$$(4.27) \qquad L = \frac{T}{m} \sqrt{\lambda_v^2 + \frac{\lambda_\gamma^2}{v^2}} - \lambda_m \beta.$$

Using (4.12-14)

$$H_o(b^1) = H_o(a^2) + H_o(a^3)$$

so (4.20) reduces to

$$L(b^1) = L(a^2) + L(a^3). \tag{4.28}$$

Equations (4.17-20) are also applicable to this problem implying that

$$\lambda_\phi(t) \equiv 0$$

and

$$H(t) \equiv 0.$$

Once again λ_ϕ may be ignored and the zero H function may be used to eliminate another multiplier.

Equation (4.21) does not apply here but in its place

$$\lambda_m(b^2) = 1.$$

This completes the list of transversality conditions which restrict the problem solution. Of course, equations (4.6-11) still may be used to determine the steering for each branch.

The determination of the times, t_c, to begin and, t_r, to end the coast during branch 3 may be accomplished in a variety of ways. For example, the entire coast may be eliminated from the problem analytically using the technique of reference 14. In any case the necessary conditions to be satisfied by the minimizing branched trajectory are

$$L(t_c) = 0$$

and

$$L(t_r) = 0.$$

AIR TRAFFIC CONTROL. The class of problems being considered in this study includes cooperative maneuvers of many aircraft. One of the most recently publicized problems of this type is the control of air traffic in the approach to large airports.

Although people are now working on exotic and far reaching plans for tomorrow's transportation needs, near term solutions for air traffic control are feasible through an optimal control approach. Whatever the approach, the objective must be to relieve the congestion by

landing large numbers of planes faster without a loss of efficiency or safety.

At the present time aircraft fly holding patterns in a "stacked" configuration represented by the cylinder in Figure 12a. Each aircraft has an altitude separation, Δh, from the adjacent aircraft and flies in constant altitude concentric circles. One by one each aircraft is brought out of the holding pattern to a "gate" from which the flight follows a fixed glide path to the runway. This approach, while desirable from a safety or reliability point of view because of its simplicity, does not take full advantage of modern computer control capabilities.

If a little flexibility is allowed so that some control over the path of each craft is available, then the problem of getting several aircraft to the gate at a given distance apart may be stated in terms of finding a minimal branched trajectory.

The general and realistic model for this problem would be three dimensional and would include dynamical equations with both pure state and state-control inequality constraints. Solutions using such a model would be difficult to obtain numerically and even more difficult to obtain in closed form. For that reason a representative model in two dimensions with kinematic constraints and no inequalities has been chosen to demonstrate the technique.

Only two aircraft will be considered and motion will be confined to a horizontal plane. The control region is shown in Figure 12b as a circle. The path of the first aircraft is represented as branch 1 and the second as branch 2. The motion of each aircraft is described by two differential equations.

Branch 1:

$$\dot{x}_1^1 = u_1^1$$

$$\dot{x}_2^1 = u_2^1$$

Branch 2:

$$\dot{x}_1^2 = u_1^2$$

$$\dot{x}_2^2 = u_2^2$$

The superscripts indicating branch number will be dropped when possible.

The initial state of the two aircraft is specified by a set of boundary conditions:

For the first aircraft:

$$g_1 = a^1 = 0$$

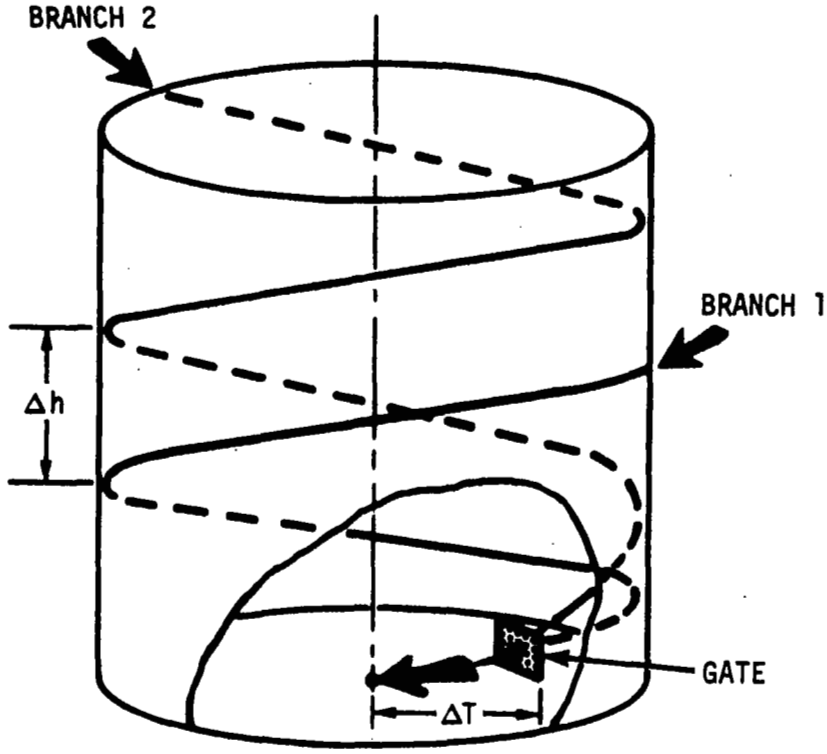

Figure 12a. Realistic Model for Air Traffic Control

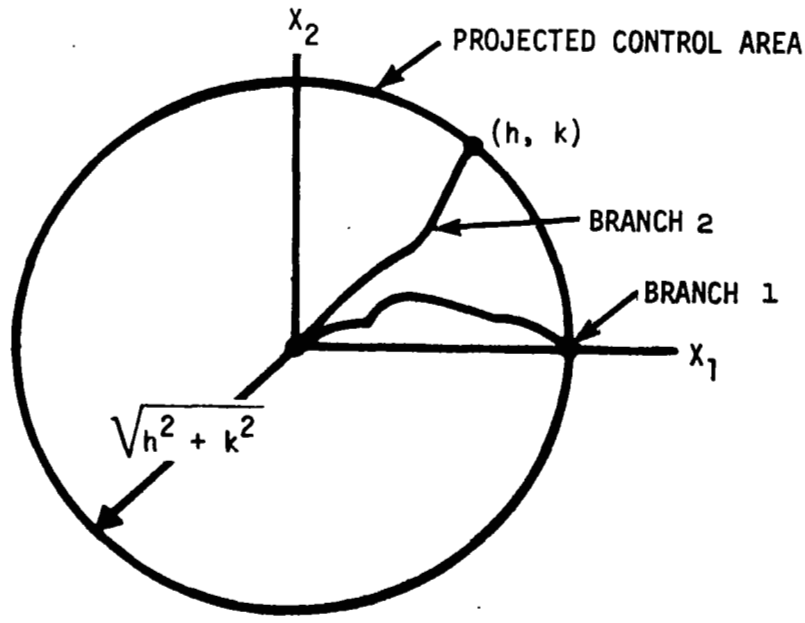

Figure 12b. Approximate Model for Projected Terminal Phase.

$$g_2 = x_1(a^1) = 0$$

$$g_3 = x_2(a^1) - \sqrt{h^2 + k^2} = 0$$

For the second aircraft:

$$g_4 = a^2 - T_o = 0$$

$$g_5 = x_1(a^2) - h = 0$$

$$g_6 = x_2(a^2) - k = 0$$

At the terminal point (or gate):

$$g_7 = b^2 - b^1 - \Delta T = 0$$

$$g_8 = x_1(b^1) = 0$$

$$g_9 = x_2(b^1) = 0$$

$$g_{10} = x_1(b^2) = 0$$

$$g_{11} = x_2(b^2) = 0$$

The gate in this case has been chosen as the origin, or the center of the control region. This merely simplifies some of the later algebra. The performance index must take into account the minimum time aspect of landing the aircraft as well as the effects of control effort for each aircraft. That is, the aircraft should reach the gate very quickly but this should not cost too much in control effort. Therefore, the weighted control effort for each aircraft is added to the time to make up the performance function.

$$J = 1/2\ K_1 \int_{a^1}^{b^1} [(u_1)^2 + (u_2)^2]dt + 1/2\ K_2 \int_{a^2}^{b^2} [(u_1)^2 + (u_2)^2]dt$$

$$+ b^1$$

For this formulation the H-function for each branch is:

$$H^j = \lambda_1{}^j\ u_1{}^j + \lambda_2{}^j\ u_2{}^j - 1/2\ K_j[(u_1{}^j)^2 + (u_2{}^j)^2]$$

$$j = 1,2$$

Hence, the Lagrange multipliers are constant and the controls are all constant.

The transversality conditions yield one piece of information, namely

$$H^1(b^1) + H^2(b^2) = 1.$$

Integrating the equations of motion and substituting the boundary values yields four algebraic equations which along with the transversality condition may be used to determine b^1 and the four controls.

$$u_1^1 = 0 \qquad u_2^1 = -(\sqrt{h^2 + k^2})/b^1$$

$$u_1^2 = h/(T_o - b^1 - \Delta T) \qquad u_2^2 = k/(T_o - b^1 - \Delta T)$$

where b^1 satisfies

$$1/2\ K_1\left[\frac{h^2 + k^2}{(b^1)^2}\right] + 1/2\ K_2\left[\frac{h^2 + k^2}{(T_o - b^1 - \Delta T)^2}\right] = 1$$

This equation is quartic in b^1 and can be solved in closed form. However, for the case of $T_o = \Delta T$ the equation reduces to a quadratic having the root

$$b^1 = \sqrt{1/2(K_1 + K_2)(h^2 + k^2)}$$

Also, the control effort

$$E_1 \equiv \int_{a^1}^{b^1} [(u_1)^2 + (u_2)^2]dt = \frac{2}{K_1 + K_2}$$

and

$$E_2 \equiv \int_{a^2}^{b^2} [(u_1)^2 + (u_2)^2]dt = \frac{2}{K_1 + K_2}\ .$$

Figure 13 shows lines of constant E_1, E_2 and b_1 plotted against the weighting factors K_1 and K_2. Since physical bounds for the control efforts establish a boundary and an upper limit on time may be given, the weighting factors may be chosen as a compromise somewhere between these bounds.

This example represents only the procedure that might be used for developing a sophisticated air terminal traffic control scheme; certainly many other factors would have to be considered but the basic approach would be very similar.

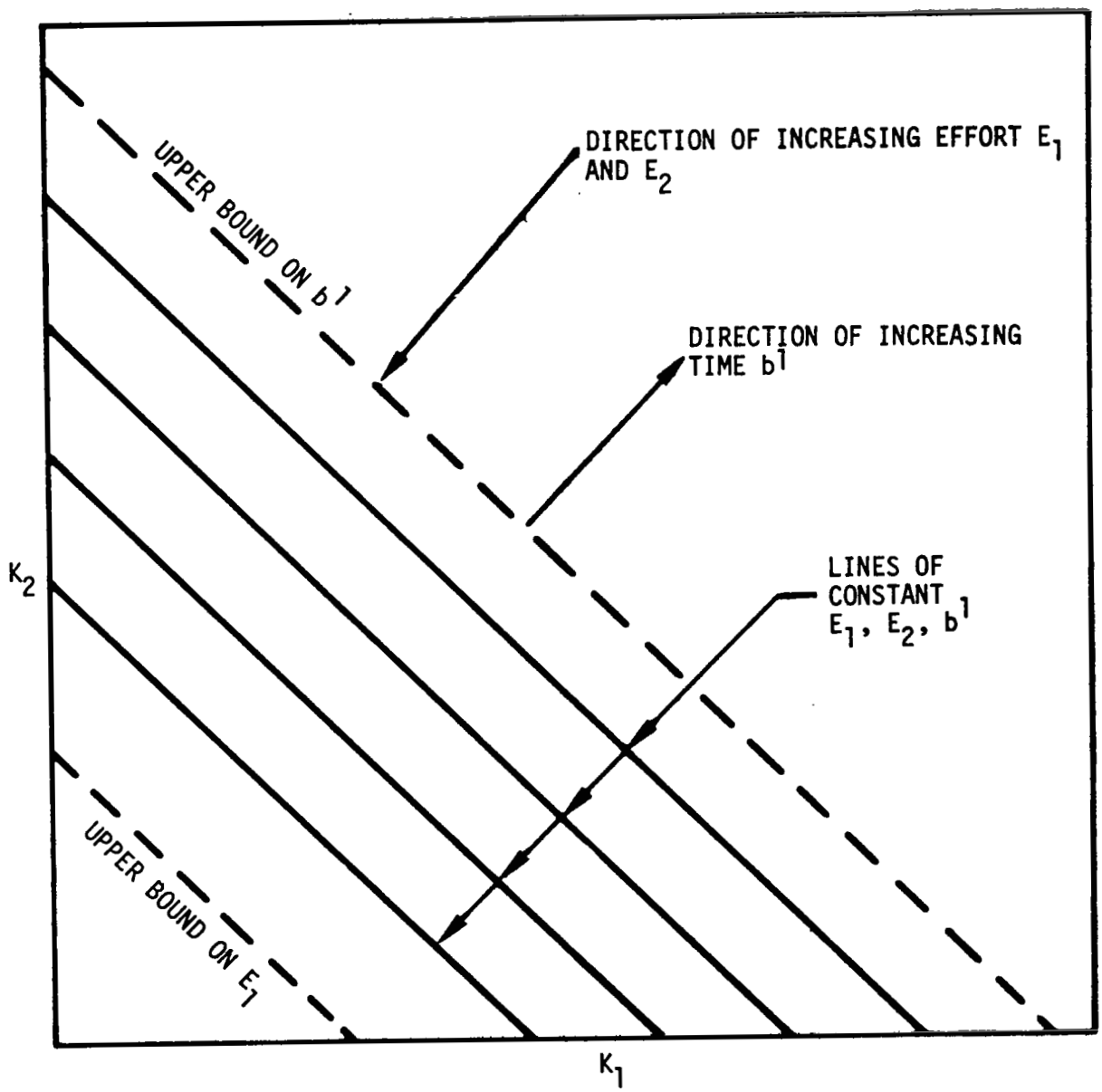

Figure 13. Performance Tradeoffs by Choice of Weighting Factors.

5.0 NUMERICAL RESULTS

Several of the applications presented in the previous section were examined numerically in order to assess the utility of branched trajectories. Optimal branched trajectories were computed for the two-payload launch case and the secondary mission optimization example. The remaining numerical effort was devoted to the lander/orbiter maneuvers.

All numerical claculations were made with TRW System Group's SDS-940 time sharing system. Two separate programs were developed to solve the branched trajectory problem. These are a numerical integration program and an iterator program. The solution procedure generally proceeded as follows.

(1) Guesses are made for unknown initial values on each branch. If a particular variable, state or Lagrange multiplier, is continuous from one branch to the next then no guess is required. Similarly if the terminal value of a multiplier is split between the initial values of that multiplier on two other branches (as in eqn. 4.12) then only one additional guess is required.

(2) With all the initial values, guessed and given, each branch is integrated numerically until some appropriate cutoff value is reached. The cutoff value may be one of the terminal conditions on the state or time or it may be a switching function. All of the terminal values are recorded along with the guesses.

(3) Each guess is then perturbed individually and a new trajectory is computed by numerical integration. Again all the terminal values are recorded along with the appropriate set of guesses. The flexibility of the time sharing system comes into play at this point. Since each perturbed trajectory is computed and examined individually, any unsuitable trajectories may be discarded and replaced by new trajectories obtained by changing the particular perturbations. Unsuitable trajectories might include those which fail to meet some cutoff conditions, those whose end states vary too greatly or insignificantly from the nominal unperturbed case and those which appear to belong to a different category of trajectories from the unperturbed case.

(4) The data from steps (2) and (3) is then used in the iterator program to compute partial derivatives of the terminal values with respect to the guesses. When the partials are known corrections for the guesses are computed. If the corrections seem unreasonably large they may be reduced by a common factor. Step (2) is then repeated with the corrected guesses. If this

results in an improvement the corrections may be applied again and again until no improvement is seen. At this point the partial derivatives may be re-used to calculate new corrections or a new set of partial derivatives may be computed by repeating step (3).

This procedure is essentially a Newton-Raphson iteration. The degree of difficulty as well as cost increases rapidly with the number of guesses. Fortunately, some of the pitfalls of this technique may be avoided in this "open loop" set up. Since the operator (engineer) may examine each trajectory prior to computing the next one, he may adjust such important parameters as perturbation step size, nominal guess values, etc.

Using this remote time sharing system other alternatives are also available to the operator. In determining an initial set of guesses for step (1) he may use a random walk procedure. That is he may arbitrarily make changes in the guesses with the purpose of reducing the largest errors in the terminal state. Usually in this procedure one guess is perturbed in the most favorable direction until the errors begin to grow, then that guess is held fixed while another is perturbed and so on.

Another technique which is sometimes helpful is to use steps (1) through (4) above but ignore one or more of the guesses and a like number of terminal constraints. Then the ignored guesses may be parameterized to satisfy the ignored constraints.

The numerical integration program used to calculate the individual trajectories employs a fourth order Runge-Kutta (ref. 15) integration scheme to simultaneously solve the Euler-Lagrange and state equations (except for the mass equation which is integrated in closed form and calculated as an explicit function of time).

Although no formal error analysis was performed on the numerical results an estimate of the truncation error (ref. 15) was obtained by re-running converged trajectories with the step size halved. If the terminal states for these two computations are respectively X and Y then the estimate of truncation error is given by:

$$\frac{1}{15}(X - Y)$$

For all of the data presented here this estimate indicated accuracy through eight significant decimal digits. It should be emphasized that this represents only an estimate of truncation error and in no way limits the size of round off error.

Although the time sharing system as described is to be highly recommended as a research tool it should not be used for production computations because of the inefficiencies of "man in the loop."

TWO PAYLOAD LAUNCH. Numerical solutions were obtained for the case of multiple payload launches discussed in section 4.0. Only two payloads were considered with one being inserted in a 180 KM circular orbit and the other in a 220 KM circular orbit. As indicated in section 4.0 five guesses are required for this problem. Two are the initial values of multipliers on branch 1 and three are the initial values of multipliers on branch 3 (see Figure 9). Branch 1 is integrated for 377.65 seconds at which time dual staging occurs. Branch 2 terminates at a given value of mass while Branch 3 stops at circular orbit velocity for the 220 KM orbit.

The data used for the various stages is listed in table 1 and represents a vehicle similar to the Saturn V. If that analogy were followed the initial state for Branch 1 would correspond to burnout conditions (exoatmospheric) for stage one of the Saturn V, Branch 1 would correspond to the trajectory of the S-II (stage two) carrying the S-IVB (stage three) and CSM (command-service module), Branch 2 would be the path of the S-IVB alone and Branch 3 the path of the CSM.

Before attempting the branched solution several conventional optimal trajectories were computed in order to gain a feeling for the performance capabilities, multiplier sensitivities and trajectory shape. Reference trajectory 1 consists of two separately computed optimal paths. The first path is that of the S-II stage carrying the S-IVB and CSM to S-II burnout after which the S-IVB carries the CSM to a 180 KM circular orbit. From that orbit the second path is for the CSM and terminates in a 220 KM circular orbit.

Reference trajectory 2 is also made up of two separate conventional optimal trajectories. The first is that of a two stage rocket terminating at the 180 KM circular orbit. The first stage is the S-II carrying the S-IVB and CSM. At the staging point the loaded CSM is discarded along with the empty S-II so that the S-IVB proceeds alone. This trajectory gives the maximum payload attainable in the 180 KM orbit if the branching occurs at S-II burnout. The second part of this reference trajectory is an optimal path for the CSM from S-II burnout to the 220 KM orbit.

Finally, the optimal branched trajectory was computed. Because of the results for Reference trajectory 2 the payload for the 180 KM orbit was prescribed at 114255.7 KG which is only 28.4 KG less than the maximum achievable. By reducing the first payload requirement this small amount the second payload was increased 156.1 KG over Reference trajectory 2. Table 2 compares the performances of the optimal branched solution and Reference trajectories 1 and 2. Notice that Reference trajectory 1 outperforms the branched solution by

TABLE 1

DATA FOR NUMERICAL EXAMPLES

Initial State

v KM/Sec	γ degrees	r KM	ϕ degrees	m KG
2.8481269	14.91	6465.036	0.	611582.1

Stage Data

Branch Number	Thrust - T Newtons	Mass Flow - β KG/Sec	Initial Mass - m KG
1	4448222	1068.2	611582.1
2	889644.3	213.1	145026.5
3	85636.8	30.5	19820.0

TABLE 2

PERFORMANCE COMPARISONS FOR DUAL PAYLOADS

Payload Number	Branched Trajectory	Reference Trajectory 1	Reference Trajectory 2
1	114255.7	109985.2	114284.1
2	13299.7	14715.5	13143.6

1415.8 KG for the second payload but pays for this with 4270.5 KG for the first payload.

An altitude-velocity plot of the branched solution is given in Figure 14. Although Reference trajectory 2 was not plotted because of the closeness to the branched trajectory its S-II burnout conditions are slightly higher and faster than those shown. This slight difference permits the branched trajectory to have better performance for the 220 KM orbit.

The CSM portion of the trajectory is given in altitude-velocity coordinates in Figure 15 along with the analogous part of Reference trajectory 1. In comparing the initial states of these two branches it is seen that for Reference trajectory 1 branch 3 starts out in a much more favorable position for the 220 KM orbit. On the other hand the cost, in terms of number one payload is very high in order to attain such an initial state for branch 3.

For this solution branching was only considered at S-II burnout. Certainly other times could have been used. In fact, it would be possible to leave the branching time free (branching to occur any time during S-IVB flight) and develop a switching function from the transversality conditions. This would be a logical next step after several fixed-branch-time trajectories have been computed.

SECONDARY MISSION OPTIMIZATION. Most of the results of this phase of the study were presented separately in reference 16. A brief summary of some of the more interesting aspects of this problem is given below.

The secondary mission case is very similar to the dual payload example except that, at the branch point, the vehicle may proceed along either branch 2 or branch 3. If no failure occurs and branch 2 is chosen then only the empty stage that was used for branch 1 is dropped. The vehicle characteristics and initial state used for this problem are the same as those given in Table 1 except that the initial mass for branch 2 is 145026.5 + 19820 = 164846.5 KG. This corresponds to carrying along the LM/CSM with the S-IVB on branch 2 but only the CSM on branch 3. The LM (lunar module) is dropped prior to Branch 3.

In order to establish some basis for comparison a conventional optimal trajectory was computed for the primary mission only (180 KM circular orbit). This trajectory produced 129805 KG payload for the primary mission. From the staging point of this solution another optimal trajectory, using the CSM only, was computed for the secondary mission (206 KM circular orbit). The payload for this mission was 13720 KG. Altitude-velocity plots for the S-II, S-IVB and CSM portions of these optimal trajectories are shown in Figures 16 and 17; the label "nominal" is used to distinguish these profiles from the optimal branched trajectories.

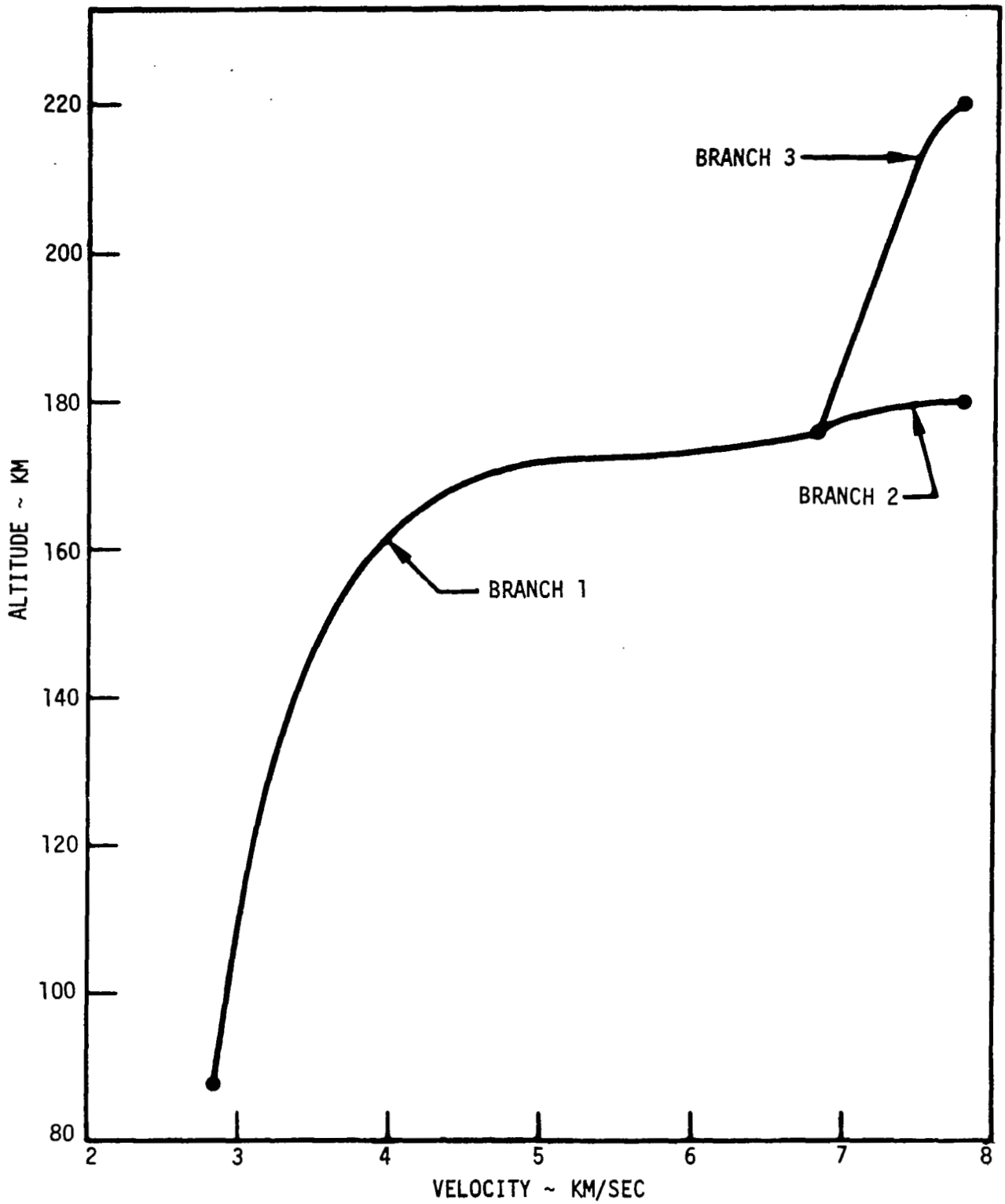

Figure 14. Altitude - Velocity Diagram for Dual Payload Optimal Branched Trajectory

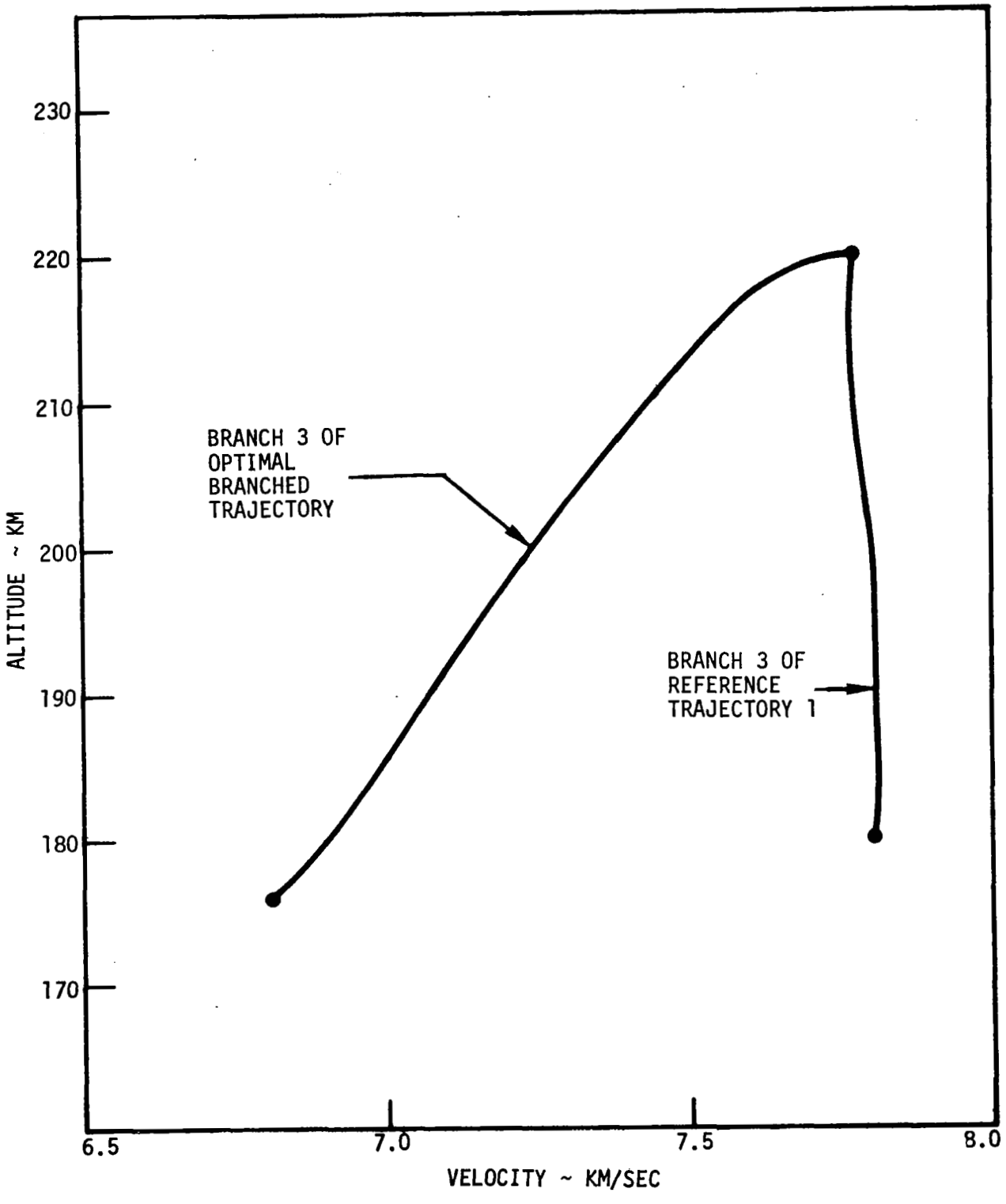

Figure 15. Comparison of Branch 3 Solutions

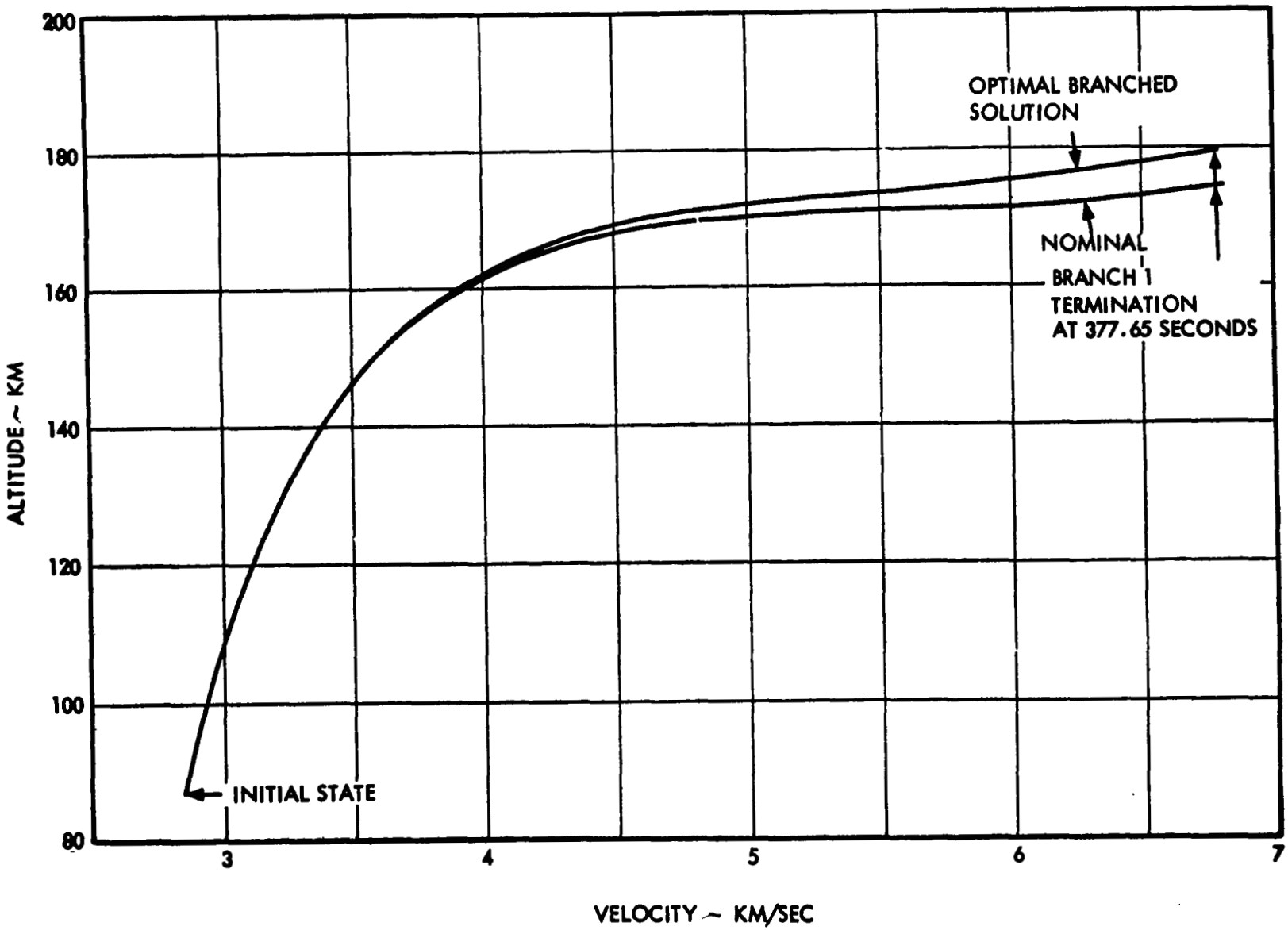

Figure 16. Altitude - Velocity Plots Comparing Branch 1 Solutions for Maximum Secondary Payload

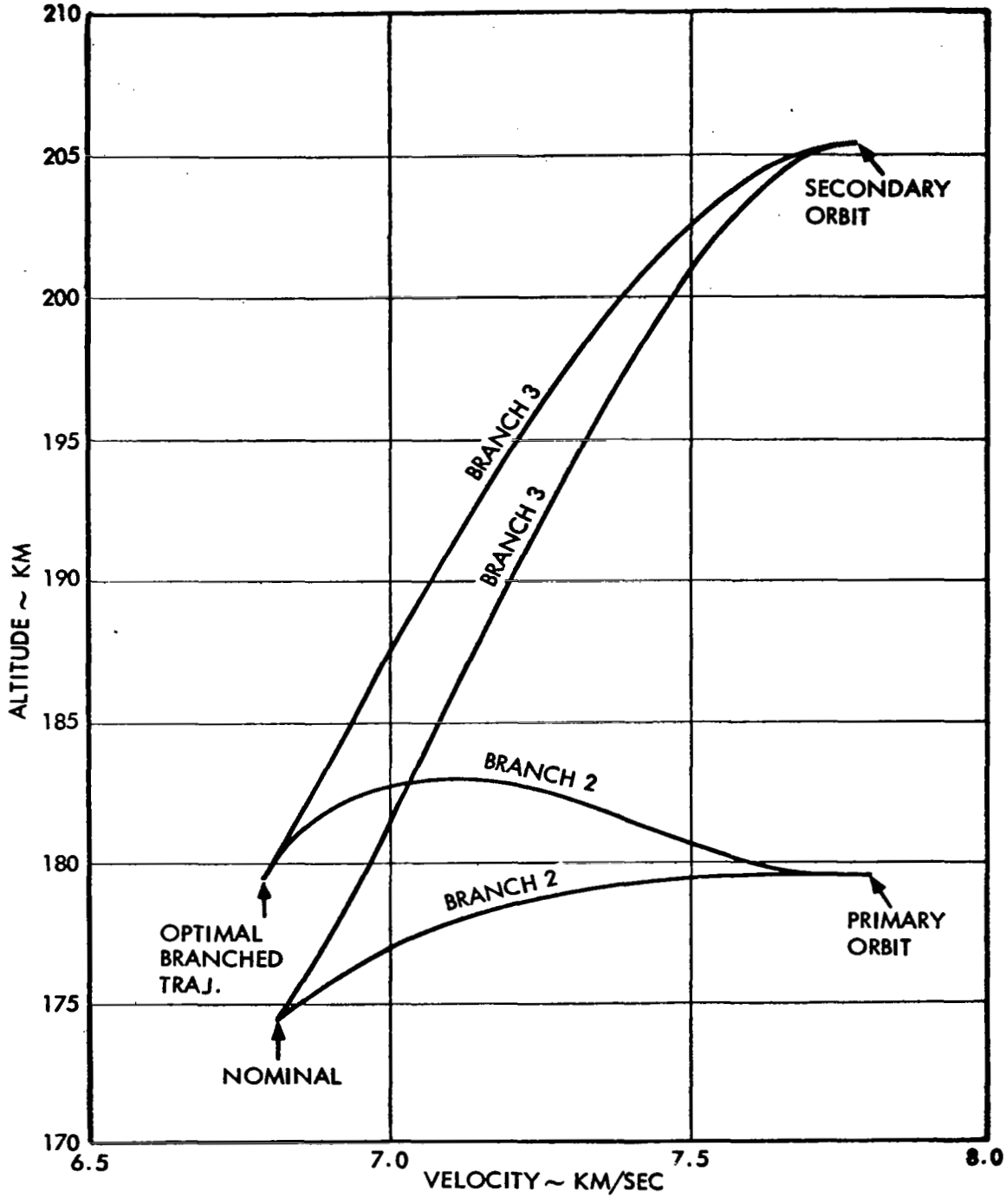

Figure 17. Altitude - Velocity Plots for Branches 2 and 3 for Maximum Secondary Payload

For the nominal trajectory 35041.3 KG of propellant was used for branch 2. This establishes a lower limit for branch 2 propellant; any amount less than 35041.3 KG will result in a loss of payload for the primary mission.

It is also possible to establish a practical upper limit for branch 2 propellant. This was accomplished by computing a conventional optimal trajectory consisting only of branches 1 and 3 with the terminal point satisfying the secondary mission circular orbit conditions. Once again, the remaining branch (2) was optimized starting at the staging point between 1 and 3 and terminating at the primary orbit. For this pair of optimal trajectories the secondary mission payload was 14182.3 KG and the propellant consumed on branch 2 was 38590.5 KG (corresponding to a primary payload of 126256 KG). Since no branched trajectory will provide more than 14182.3 KG secondary payload, it would be wasteful to attempt to burn more than 38590.5 KG of propellant on branch 2.

After the maximum payload for the nominal case was established it was possible to consider secondary mission optimization by specifying some payload for the primary mission less than the maximum. The number 129168 KG was chosen, thus allowing 637 KG more fuel to be consumed during the S-IVB flight. Figure 16 shows that this additional propellant permits a higher trajectory for the S-II (branch 1) which, in turn, places the branch point in a position more favorable to the secondary mission. As a result the branched solution provides 14000 KG payload for the secondary mission, an increase of 280 KG over the nominal. By expending 637 KG more propellant in branch 2 we can decrease the propellant in branch 3 by 280 KG which could spell the difference between partial success and complete failure if an abort is required at S-IVB ignition.

Figure 18 gives a comparison of control histories for the optimal branched solution and the nominal. The marked difference in control for branch 2 is due to the relative locations of the branch point with respect to the primary orbit. On the optimal branched solution this point falls just above 180 KM while on the nominal staging takes place at 175 KM, 5 KM below the desired orbit.

To this point only the circumstance of an abort occurring at S-IVB ignition has been considered. This event was chosen because of its critical nature and the optimal branched trajectory was designed on the assumption that failure might only occur at this point. Obviously other branch points could be included in the analysis although numerical difficulty increases, because of increased dimensionality, with the addition of each branch. Also, in the case of multiple secondary branches the performance criterion would have to include weighted performances of each branch.

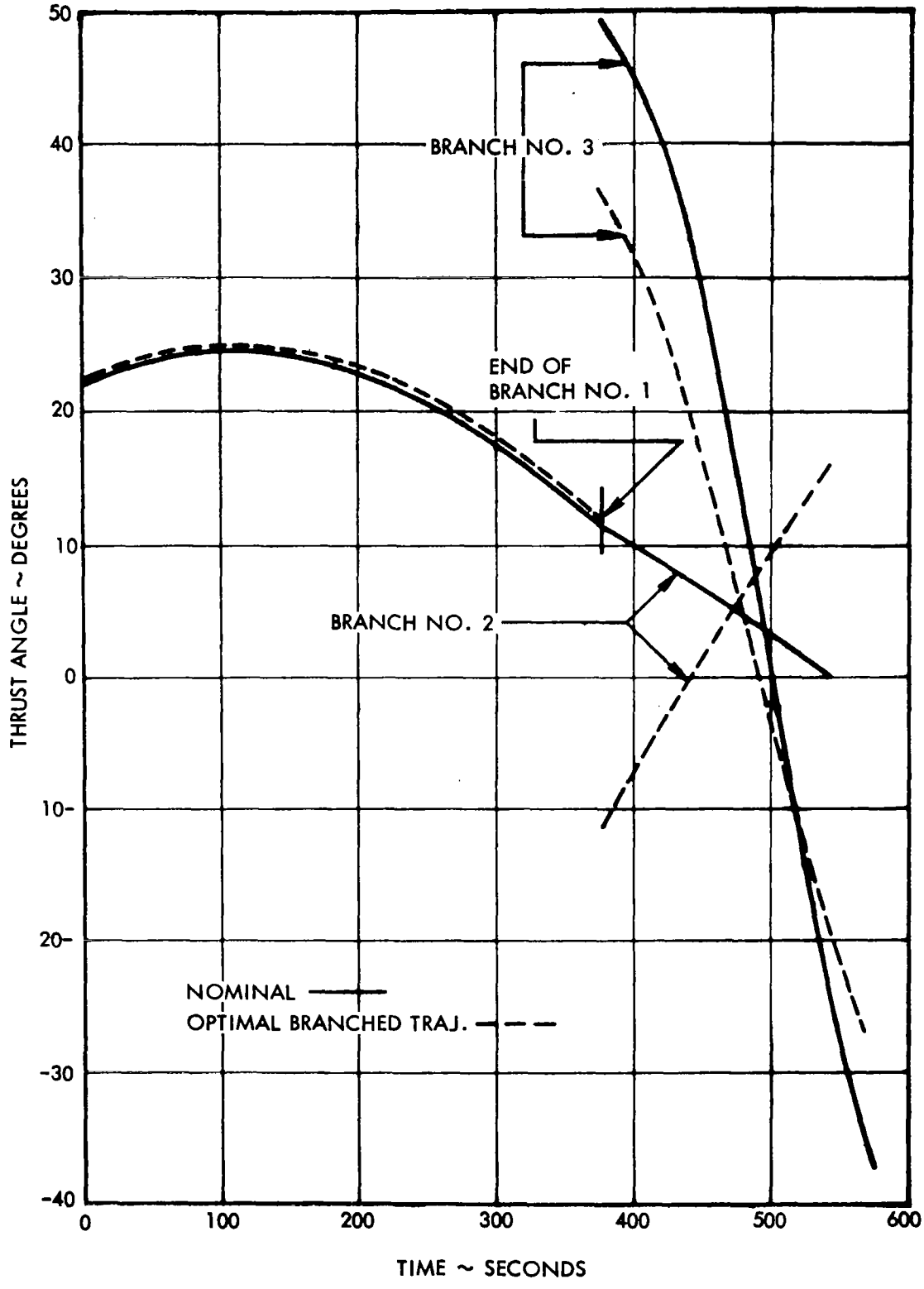

Figure 18. Optimal Control for Branched and Nominal Solutions for Maximum Secondary Payload

Although the branched trajectories considered here were not specifically designed for an abort occurring after S-IVB ignition, they do possess some capability for that case. To investigate the performance behavior resulting from such an occurrence, two optimal abort trajectories to the secondary orbit were calculated starting 47.35 seconds after S-IVB ignition. The first case was initiated on the nominal trajectory while the second abort departed from branch 2 of the branched solution.

The latter provided 58 KG more payload than the former, but even more important, it provided 615 KG more payload than the optimal branched solution with an abort occurring at S-IVB ignition. Thus, while later aborts from the branched trajectory may not be optimal, they are also less likely to require optimality because of a natural increase in payload capability.

Figure 19 is an altitude-velocity plot of the two abort trajectories. The abort from the branched solution has an initial altitude advantage, but a slight disadvantage in velocity and flight path angle. If the abort occurs late enough these disadvantages eventually overcome the edge in altitude as shown in Figure 20.

The secondary mission chosen here is truly just that. An alternate choice could have been true abort where the second mission would represent re-entry conditions instead of the 220 KM circular orbit. The abort case should yield to the same analysis and numerical techniques.

BRANCHED LANDER/ORBITER MANEUVERS. The latter part of this study was devoted to a numerical investigation of optimal branched lander/orbiter maneuvers as shown in Figure 11. This problem proved considerably more difficult than the previous two numerical examples and a solution was not obtained. Part of the trouble with this case is the necessity of including a coasting period in branch 2. This, combined with the sensitivity imposed by the near zero terminal velocity for branch 2, provided an obstacle not easily overcome especially with the simplified iteration scheme used.

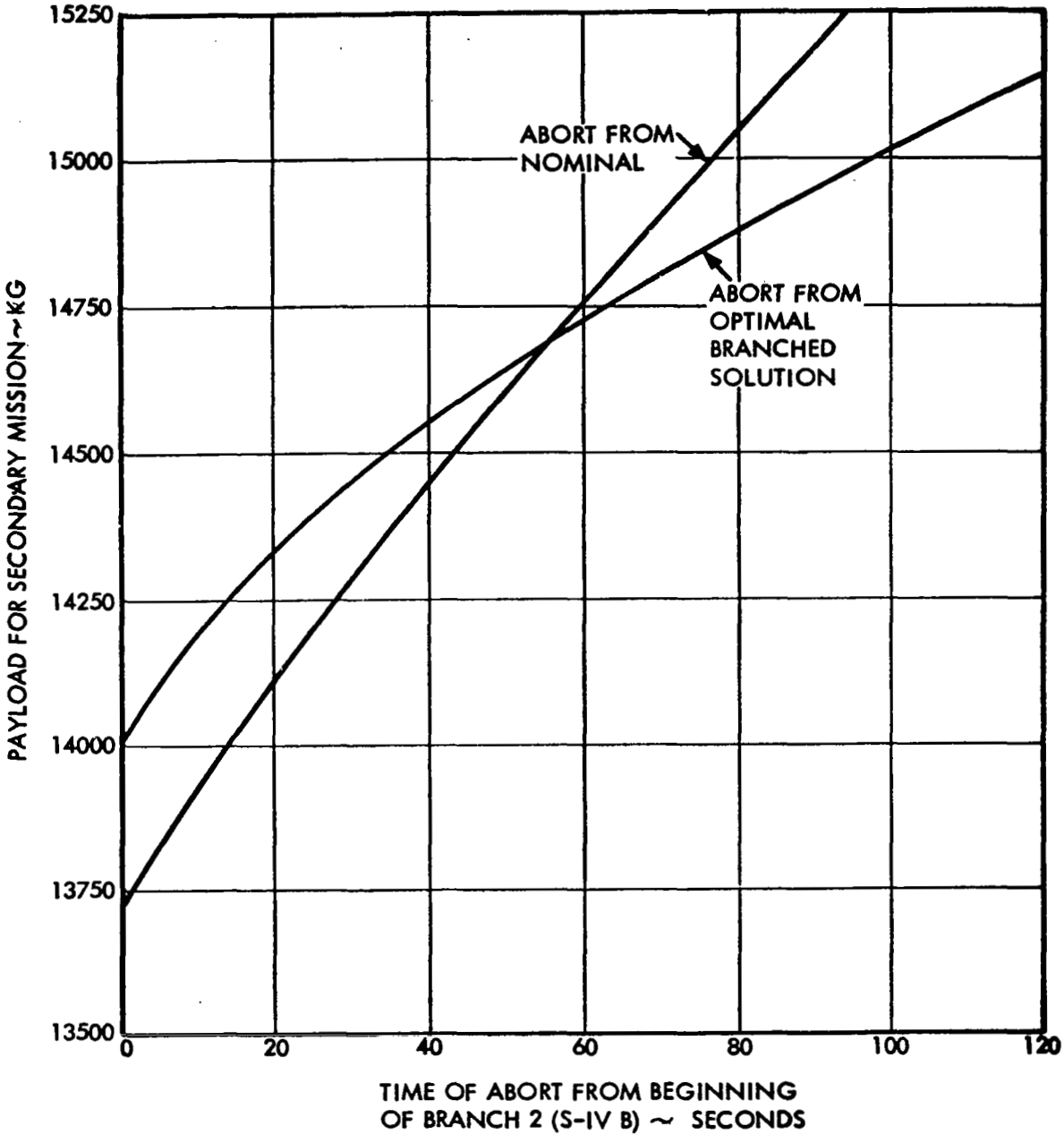

Figure 19. Altitude - Velocity Plot for Abort from Nominal and Branched Solution 47.35

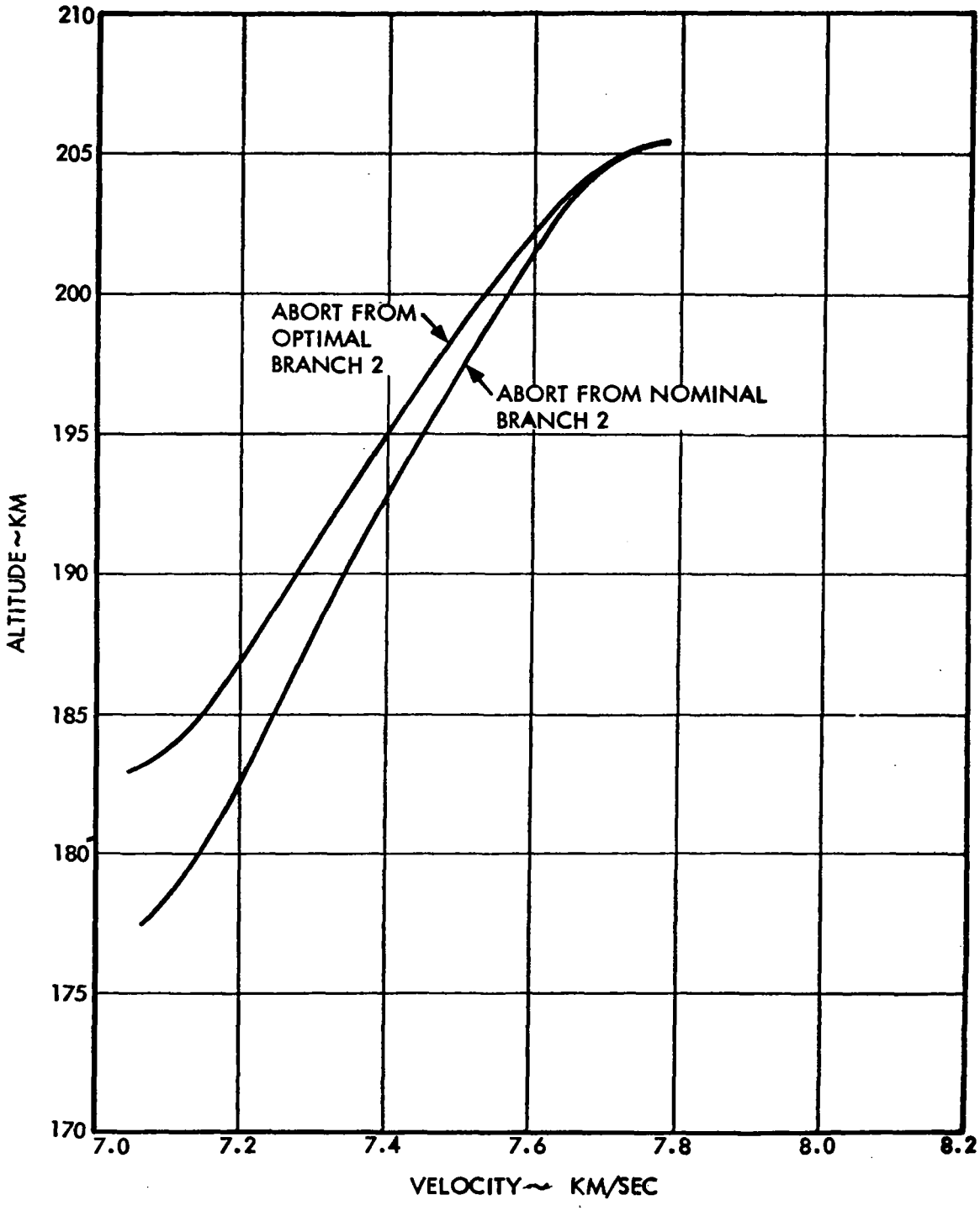

Figure 20. Payload vs. Time of Abort

REFERENCES

1. Bliss, G. A. and Mason, M.,"A problem of the calculus of variations in which the integrand is discontinuous", Trans. of the Am. Math. Soc., vol. 7 (1906), pp. 325-336

2. Roos, C. F.,"A general problem of minimizing an integral with discontinuous integrand", Trans. of the Am. Math. Soc., vol. 30 (1929), pp. 58-70

3. Graves, L. M.,"Discontinuous solutions in space problems of the calculus of variations", Am. J. of Math., vol. 52 (1930), pp. 1-28

4. Sinclair, M. E.,"Concerning a compound discontinuous solution in the problem of the surface of revolution of minimum area", Annals of Math., (2), vol. 10 (1909), pp. 55-80

5. Denbow, C. H.,"A generalized form of the problem of Bolza", Ph. D. dissertation, Univ. of Chicago (1937)

6. Hestenes, M. R.,"Generalized problem of Bolza in the calculus of variations", Duke Math. J., vol. 5 (1939), pp. 309-324

7. Hunt, R. W. and Andrus, J. F.,"Optimization of trajectories having discontinuous state variables and intermediate boundary conditions", presented at joint AIAA-IMS-SIAM-ONR Symposium on Control and System Optimization, Monterey, California (January 27-29, 1964).

8. Mason, J. D., Dickerson, W. D. and Smith, D. B.,"A variational method for optimal staging", AIAA J., vol. 3, no. 11 (1965), pp. 2007-2012

9. Boyce, M.G. and Linnstaedter, J. L., "Necessary Conditions for a Multistage Bolza-Mayer Problem Involving Control Variables and Having Inequality and Finite Equation Constraints," NASA TM X-53292 (July 12, 1965).

10. Burns, R. E., "A Review of Some Existing Literature Concerning Discontinuous State Variables in the Calculus of Variations," NASA TN D-3450 (June 1966).

11. Vincent, T. L., "Multisegmented Optimal Trajectories," NASA CR-1103 (June 1968).

12. Warga, J.,"The reduction of certain control problems to an 'Ordinary Differential' type", SIAM Review, vol. 10 (1968), pp. 219-222

13. Hestenes, M. R.,"Calculus of Variations and Optimal Control Theory", John Wiley and Sons, Inc., New York (1968)

14. Mason, J. D.,"Transformations and discontinuities for optimal space trajectories", Ph. D. dissertation, Univ. of Arizona (1968)

References (continued)

15. Hildebrand, F. B., "Introduction to Numerical Analysis," McGraw-Hill Book Company, New York (1956).

16. Mason, J. D., Smith, D. B. and Dickerson, W. D.,"Secondary mission optimization", AAS paper no. 68--138, presented at the AAS/AIAA Astrodynamics Specialist Conference, Jackson, Wyoming (September 1968)

NASA-Langley, 1969 —— 30 CR-1331